State-of-the-Art Review

Comparison between Distance Functions for Approximate Bayesian Computation to Perform Stochastic Model Updating and Model Validation under Limited Data

Adolphus Lye[1]; Scott Ferson[2]; and Sicong Xiao[3]

Abstract: The paper reviews the distance functions that have been or could be used to perform stochastic model updating via approximate Bayesian computation, namely: (1) Euclidean distance; (2) Bhattacharyya distance; (3) Bray–Curtis distance; and (4) 1-Wasserstein distance functions. For each of these distance functions, details on their mathematical formalism and implementation are provided along with an evaluation of their respective advantages and disadvantages illustrated though a numerical study. Subsequently, to provide a basis for comparison in the stochastic model updating performance by the respective distance functions, two case studies in the form of model validation problems are presented. The first problem is based on the 2014 NASA-LaRC Multidisciplinary Uncertainty Quantification Challenge. The second problem is based on the 2008 thermal problem presented by Sandia National Laboratories. Both problems provide a relatively complex and realistic setting to assess the strengths and robustness of each distance function in performing approximate Bayesian computation under polymorphic uncertainty and limited data for a one-dimensional output space. The comparison will be done based on the following: (1) the precision of the inference results on the inferred parameters; and (2) the precision of the corresponding stochastic model output against a set of validation data. **DOI: 10.1061/AJRUA6.RUENG-1223.**

Introduction

Within the field of modern engineering, the need for numerical models and simulations have grown significantly in recent years in such a manner that they are seemingly irreplaceable in the study of engineered systems and components (Bi et al. 2023). This characteristic is especially so in cases whereby it becomes challenging to obtain data through experimental campaigns resulting in the limited availability of experimental data (Lye et al. 2022c, 2023b). The numerical models should ideally represent the physical system in a manner such that there is no discrepancy between the resulting simulated model output and the experimental measurement.

However, such discrepancy exists in reality because the simulated output by the numerical models do not take into account the effects of the measurement "noise" (Helton 1997; Helton et al. 2004) as well as the other sources of uncertainties such as the model form uncertainty and the model parameter uncertainty. Such uncertainties are classified into two broad categories (Oberkampf et al. 2004; Roy and Oberkampf 2011): (1) aleatory uncertainty and (2) epistemic uncertainty. Aleatory uncertainty refers to the fluctuations and the statistical uncertainty of a given variable due to its inherent randomness and variability. Such uncertainty is irreducible and is usually described with a probability distribution. Epistemic uncertainty, conversely, refers to the lack of knowledge about the parameter(s) or variable(s) of interest. Unlike in the case of aleatory uncertainty, epistemic uncertainties are reducible with increased study or observations, and such uncertainties are often conceptualized as a fixed value within a bounded set whose breadth reflects the level of knowledge on the parameter.

Model updating techniques have been developed to calibrate the model parameters, and hence the model itself, such that the discrepancy between the simulated model output and the experimental measurement is minimized (i.e., as close to zero as possible) (Mottershead and Friswell 1993; Mottershead et al. 2021). The process of model updating can also be viewed as model calibration and has been widely implemented in model verification and validation (Worden 2001; Simoen et al. 2015). Model verification refers to the process of ensuring that the numerical model is consistent and its solution agrees with the underlying physics-based or mathematical equations. Model validation refers to the process of evaluating how accurate the numerical model represents the physical system being studied based on physical experiments conducted from the perspective of the intended user(s) (Bi et al. 2023). The latter concept serves as the basis of study of the paper. Broadly speaking, model updating can be categorized into two distinct types (Lye et al. 2021): (1) deterministic model updating; and (2) stochastic model updating.

In a deterministic model updating framework, the calibration of the model is done without accounting for any form of uncertainty associated with the inferred model parameter(s). Through such an approach, the model calibration procedure is performed based on a single set of test data (Patelli et al. 2017). This yields a single set of crisp values on the inferred model parameter(s) resulting in a single model prediction with maximum fidelity given the single set of test data. Examples of such approaches toward model updating include the following: (1) the linear least-squares minimization; and (2) sensitivity-based model updating (Patelli et al. 2017). Although the deterministic model updating approach can be

[1]Research Fellow, Singapore Nuclear Research and Safety Initiative, National Univ. of Singapore, 1 CREATE Way, Singapore S138602 (corresponding author). ORCID: https://orcid.org/0000-0002-1803-8344. Email: snrltsa@nus.edu.sg

[2]Professor and Director of the Institute for Risk and Uncertainty, Institute for Risk and Uncertainty, Univ. of Liverpool, Liverpool L697ZF, UK. Email: ferson@liverpool.ac.uk

[3]Senior Research Fellow and Principal Investigator, Singapore Nuclear Research and Safety Initiative, National Univ. of Singapore, 1 CREATE Way, Singapore S138602. Email: snrxs@nus.edu.sg

Note. This manuscript was published online on March 18, 2024. Discussion period open until August 18, 2024; separate discussions must be submitted for individual papers. This paper is part of the ***ASCE-ASME Journal of Risk and Uncertainty in Engineering Systems, Part A: Civil Engineering***, © ASCE, ISSN 2376-7642.

systematic in its implementation, its disadvantages include the following: (1) the issue of high computational costs when performing global optimizations on the inferred parameter(s); (2) lack of accounting for the uncertainty that can be attributed to the test data or the model form; and (3) provision of a single solution to the updated model predictions and the inferred parameter(s) that neglects other possible solutions with equal importance. To overcome such limitations, the stochastic model updating framework was developed.

In a stochastic model updating framework, the model calibration procedure is done while accounting for the presence of both the aleatory and epistemic uncertainties (i.e., polymorphic uncertainty) (Gotz et al. 2015; Graf et al. 2015; Drieschner et al. 2021). Imprecise probability models are required to model the inferred parameter(s) whose uncertainty can be aleatory but the uncertainty over its distribution hyperparameters (i.e., the mean and variance parameters) can be epistemic. Examples of such imprecise probability models include (1) the probability-box (Ferson et al. 2003), (2) evidence theory (Yager et al. 1994), and (3) fuzzy-probability model (Zadeh 1965; Beer 2009). Unlike the deterministic approach, a probabilistic approach does not provide point estimates to the inferred parameters, but rather as intervals or probability distributions. This approach yields a set of probabilistic model predictions that are able to illustrate the uncertainty associated with the given observations (Lye 2023).

One of the most well-established stochastic model updating approaches is the Bayesian model updating framework (Beck and Katafygiotis 1998; Katafygiotis and Beck 1998; Lye et al. 2021), which will serve as the context of the paper. The approach allows for the subjective prior information of the analyst to be integrated with observations or experimental data to update the knowledge on the inferred model parameters of interest as a posterior. In most cases, the inference on the epistemic model parameters is done numerically via sampling, which can become computationally expensive when the number of inferred model parameters becomes high (e.g., 20 parameters) (Lye et al. 2021). For this reason, the approximate Bayesian computation approach was developed to reduce the computational cost by providing kernel density estimates on the likelihood function, which is built upon certain statistics of the data set (Turner and Zandt 2012; Beaumont et al. 2002; Marin et al. 2012; Zhao et al. 2022a).

In most cases, however, the provision of Kernel Density Estimates on the likelihood function becomes challenging due to the high costs and duration of the data collection procedure. Under this circumstance, the data obtained might not be sufficient in size to form a smooth kernel density function and, therefore, a smooth posterior distribution over the inferred model parameters (Bi et al. 2019; Zhao et al. 2022a). To overcome such issue, Bi et al. (2019) proposed the implementation of a distance-based approximate Gaussian likelihood function (Bi et al. 2019) that uses distance functions to quantify the dissimilarity between the distribution of the simulated model output and the experimental data. Examples of such distance functions include: (1) the Euclidean distance, (2) the Bhattacharyya distance, (3) the Bray–Curtis distance, and (4) the 1-Wasserstein distance, about which details are presented.

Although recent research efforts have been dedicated toward developing such distance functions for approximate Bayesian computation as well as their implementation in different engineering problems (Zhao et al. 2022a), there has yet to be any investigation toward comparing the model validation performance between the different distance functions implemented in approximate Bayesian computing. The objectives of the paper are as follows: (1) to review and evaluate the state-of-the-art distance functions implemented for approximate Bayesian computation; (2) to compare the model validation performance between the reviewed distance functions under complex settings; and (3) to provide accessible codes to the readers who are new to the concept of approximate Bayesian computation as its applications toward model validation.

The section "Bayesian Model Updating" reviews the concept of Bayesian model updating and the approximate Bayesian computation framework; the section "Review of the Distance functions" reviews and evaluates the Euclidean, Bhattacharyya, Bray–Curtis, and the 1-Wasserstein distance functions implemented to perform the Approximate Bayesian Computation; the section "Case Study 1: The Nasa-Larc Multidisciplinary UQ Challenge" presents the first model validation case study based on the 2014 NASA-LaRC Multidisciplinary UQ Challenge (Crespo et al. 2014); the section "Case Study 2: The Thermal Problem" presents the second model validation case study based on the 2008 thermal problem (Hills et al. 2008); and the section "Conclusions" provides a summary and conclusion.

Bayesian Model Updating

Conceptual Framework

A standard approach toward stochastic model updating in engineering applications is Bayesian model updating (Lye et al. 2021), which is based on Bayes' rule

$$P(\boldsymbol{\theta}|\boldsymbol{D}, M) = \frac{P(\boldsymbol{D}|\boldsymbol{\theta}, M) \cdot P(\boldsymbol{\theta}|M)}{P(\boldsymbol{D}|M)} \tag{1}$$

where $\boldsymbol{\theta}$ denotes the row vector of the inferred parameters; $\boldsymbol{D}$ denotes the row vector of observations/measurements used to update our knowledge on $\boldsymbol{\theta}$; and M denotes the model as a function of $\boldsymbol{\theta}$ that is used to predict the measured quantity. The terms expressed in Eq. (1) are:

- $P(\boldsymbol{\theta}|M)$ is the prior distribution quantifying our knowledge of $\boldsymbol{\theta}$ before obtaining any measurements;
- $P(\boldsymbol{D}|\boldsymbol{\theta}, M)$ is the likelihood function reflecting the measurement error and quantifying the degree of agreement between the observed measurements and the model prediction by M;
- $P(\boldsymbol{\theta}|\boldsymbol{D}, M)$ is the posterior distribution which quantifies our updated knowledge of $\boldsymbol{\theta}$ after accounting for the observed measurements $\boldsymbol{D}$; and
- $P(\boldsymbol{D}|M)$ is the normalizing constant to ensure the posterior sums to one.

In the interest of the length of the paper, readers may refer to Chapter 2 of Lye (2023) for in-depth details to the previously listed terms, what they mean, and how they relate in the engineering context.

In general, due to the complexity in computing $P(\boldsymbol{D}|M)$, especially under high dimensions, and because the evidence term is a numerical constant, the posterior $P(\boldsymbol{\theta}|\boldsymbol{D}, M)$ can be simplified as follows:

$$P(\boldsymbol{\theta}|\boldsymbol{D}, M) \propto P(\boldsymbol{D}|\boldsymbol{\theta}, M) \cdot P(\boldsymbol{\theta}|M) \tag{2}$$

However, due to $P(\boldsymbol{\theta}|\boldsymbol{D}, M)$ now being un-normalized, direct sampling via the standard Monte Carlo method becomes inapplicable. This challenge motivated the development of the Markov chain Monte Carlo (MCMC) methods, which include: (1) the Metropolis–Hastings sampler (Hastings 1970); (2) the Gibbs sampler (Gelfand and Smith 1990; Gilks and Wild 1992); (3) the affine-invariant ensemble sampler (Goodman and Weare 2010); (4) the transitional Markov chain Monte Carlo (TMCMC) sampler (Ching and Chen 2007; Betz et al. 2016); (5) the transitional ensemble Markov chain Monte Carlo (TEMCMC) sampler (Lye et al. 2022a);

and (6) the sequential ensemble Monte Carlo (SEMC) sampler (Lye et al. 2023a, c, 2022b).

For the case studies presented in the paper, the state-of-the-art TEMCMC sampler will be employed (Lye et al. 2022a). The algorithm is a variant of the TMCMC sampler developed by Ching and Chen (2007) where the Metropolis-Hastings sampler is replaced with the affine-invariant ensemble sampler as the MCMC kernel to improve the mixing performance of the sampler and to overcome the computational challenge of sampling from a highly skewed and anisotropic posterior. Like the TMCMC sampler, the TEMCMC sampler generates samples from $P(\boldsymbol{\theta}|\boldsymbol{D}, M)$ via a series of intermediate distributions known as "transitional" distributions P^j, defined as (Ching and Chen 2007)

$$P^j \propto P(\boldsymbol{D}|\boldsymbol{\theta}, M)^{\beta_j} \cdot P(\boldsymbol{\theta}|M) \tag{3}$$

where $j = 0, 1, \ldots, m$ is the iteration number; and β_j = tempering parameter such that $\beta_0 = 0 < \beta_1 < \ldots < \beta_m = 1$.

A summary to the procedure implemented by the TEMCMC sampler in generating N samples from $P(\boldsymbol{\theta}|\boldsymbol{D}, M)$ is as follows: at iteration $j = 0$, a total of N realizations of $\boldsymbol{\theta}$ are first obtained from the prior $P(\boldsymbol{\theta}|M)$ via direct Monte Carlo sampling. At iteration $j = 1$, the samples are updated according to the distribution P^j using the affine-invariant ensemble sampler based on the selected samples from the distribution. After, the algorithm proceeds to iteration $j = j + 1$, and the procedure of updating the samples according to P^j is repeated until the terminal iteration $j = m$, where P^j corresponds to the posterior $P(\boldsymbol{\theta}|\boldsymbol{D}, M)$. In the interest of the length of the paper, the readers are referred to Lye et al. (2022a) for full details on the TEMCMC algorithm and its implementations.

Approximate Bayesian Computation

An important aspect of the Bayesian model updating framework is the likelihood function $P(\boldsymbol{D}|\boldsymbol{\theta}, M)$ because it not only serves to model the variation (i.e., measurement error) associated with the observations $\boldsymbol{D}$ but also the degree of agreement between the observed measurements $\boldsymbol{D}$ and the predicted/simulated observations $\boldsymbol{D}_{\text{sim}}$ where (Lye et al. 2021)

$$\boldsymbol{D}_{\text{sim}} = M(\boldsymbol{\theta}) \tag{4}$$

In essence, the likelihood function serves to provide the statistical weights on the samples of $\boldsymbol{\theta}$ based on the level of "discrepancy" between the resulting $\boldsymbol{D}_{\text{sim}}$ and $\boldsymbol{D}$. In most applications, it is assumed that the individual measurements are mutually independent of one another and that the variation follows a zero-mean normal distribution (Lye et al. 2021; Zhao et al. 2022a). The full likelihood function $P(\boldsymbol{D}|\boldsymbol{\theta}, M)$ is defined as:

$$\begin{aligned} P(\boldsymbol{D}|\boldsymbol{\theta}, M) &= \prod_{k=1}^{N_{\text{obs}}} P(\boldsymbol{D}_k|\boldsymbol{\theta}, M) \\ &= \prod_{k=1}^{N_{\text{obs}}} \frac{1}{\varepsilon_o\sqrt{2\pi}} \cdot \exp\left[-\frac{(\boldsymbol{D}_k - M(\boldsymbol{\theta}))^2}{2\varepsilon_o^2}\right] \end{aligned} \tag{5}$$

where N_{obs} = number of observations; and ε_o = standard deviation of the measurement variation.

Practically speaking, the analytical likelihood function may not necessarily be available in general (Zhao et al. 2022a). Under such scenario, the probability density function (PDF) to $P(\boldsymbol{D}|\boldsymbol{\theta}, M)$ needs to be estimated and evaluated for each sample realization of $\boldsymbol{\theta}$. There are two challenges to such approach. First, the total number of sample realizations of $\boldsymbol{\theta}$ is generally large (e.g., $N =$ 1,000) when performing a full Bayesian model updating procedure and computation (Patelli et al. 2015; Safta et al. 2015). This process can become computationally expensive and inefficient, especially when the computational cost per model evaluation becomes significant. Second, a single PDF estimation through standard techniques such as the kernel density estimates (KDE) would require many realizations of $\boldsymbol{D}_{\text{sim}}$ [i.e., see Eq. (4)] which may be difficult to achieve due to the issue highlighted in the first point. Conversely, even if an analytical formula to $P(\boldsymbol{D}|\boldsymbol{\theta}, M)$ is available [e.g., Eq. (5)], a large number of model evaluations is required, which can also become a computationally expensive procedure in cases when the model M is complex with high-dimensional parameter inputs and features (Bi et al. 2019). To overcome such problems, one can turn to the approximate Bayesian computing (ABC) approach (Abdessalem et al. 2019; Fang et al. 2019; Park and Grandhi 2012; de Carlo et al. 2016; Turner and Zandt 2012).

Under the ABC framework, the full likelihood function is replaced with an approximate function that still retains information pertaining to the observed $\boldsymbol{D}$ and the realizations of $\boldsymbol{D}_{\text{sim}}$ by $\boldsymbol{\theta}$ via Eq. (4) (Turner and Zandt 2012). Some examples to the approximate functions implemented in the literature include the Gaussian (Rocchetta et al. 2018a), Epanechnikov (Beaumont et al. 2002), and the Sharp (Safta et al. 2015) functions. In essence, the approximate likelihood function should still be capable of returning a high value when the discrepancy between that statistics of $\boldsymbol{D}$ and $\boldsymbol{D}_{\text{sim}}$ and a small value when such discrepancy is large. Such discrepancy can be quantified using a distance function, which can be implemented within the approximate likelihood function (i.e., distance-based ABC). This progression leads to the development of the distance-based approximate Gaussian likelihood function defined as (Bi et al. 2019):

$$P(\boldsymbol{D}|\boldsymbol{\theta}, M) \propto \exp\left[-\frac{d(\boldsymbol{D}, \boldsymbol{D}_{\text{sim}})^2}{\varepsilon^2}\right] \tag{6}$$

where $d(\cdot)$ is the distance function; and ε is referred to as the width factor. It was previously determined empirically, through a series of numerical model calibration experiments in Patelli et al. (2015), that the specific range of ε should lie in the interval of $[10^{-3}, 10^{-1}]$ (Bi et al. 2019). However, note that the range does not apply uniformly to all the distance functions considered, as demonstrated in the case studies presented later in the paper. Note that a smaller value of ε leads to a more peaked posterior distribution, which may increase the computation requirements for convergence, whereas a larger value of ε would reduce such computation requirement but at the expense of the convergence of the estimates to the true values, providing a basis to the choice of ε in the case studies presented in the later sections of the paper.

The choice of d is also crucial because it needs to be able to effectively reflect the statistical difference between $\boldsymbol{D}$ and $\boldsymbol{D}_{\text{sim}}$ for a given realization of $\boldsymbol{\theta}$. In turn, it would have an impact on the Bayesian model updating and the subsequent model validation results. Considering such importance, the next section presents a review to some of the distance functions that have been implemented in the literature and provides an evaluation to their respective pros and cons.

To conclude the section, readers are referred to Marin et al. (2012) and Lintusaari et al. (2017) for detailed information to the ABC algorithm along with the mathematical and numerical proofs to the approach.

Review of the Distance Functions

The objective of the distance functions is to quantify the statistical difference between any two statistical objects x_1 and x_2 in the

form of samples, random variables, or probability distributions. A general distance function d should have these four mathematical properties (Frechét 1906)

1. Non-negativity: $d(x_1, x_2) \geq 0$;
2. Symmetry: $d(x_1, x_2) = d(x_2, x_1)$;
3. Triangle inequality: $d(x_1, x_2) \leq d(x_1, y) + d(y, x_2)$; and
4. Identity of indiscernibles: $d(x_1, x_2) = 0$, only if $x_1 = x_2$.

In the context of ABC, the two statistical objects of interest are the vectors of observed/measured data $\boldsymbol{D}$ and the model prediction $\boldsymbol{D}_{\text{sim}}$.

Other functions can also be useful that do not satisfy all of the properties, including the following: (1) the quasi metric; (2) the semi metric; and (3) the pseudo metric. The quasi metric is a distance that satisfies all conditions except for the symmetric property (Wilson 1931; Bukatin et al. 2017). Examples include the Kullback–Leibler divergence (Kullback and Leibler 1951; Kullback 1997) and the Hausdorff distance (Rockafellar and Wets 2010). The semi metric is a distance that satisfies all conditions except for the triangle inequality (Chrzaszcz et al. 2018; Jachymski and Turobos 2020). Examples include the Bhattacharyya (Bhattacharyya 1943, 1946) and the Bray–Curtis distances (Bray and Curtis 1957; Ricotta and Podani 2017). Finally, the pseudo metric is a distance that satisfies all conditions except for the identity of indiscernibles (Smyth 1988; Steen and Seebach 1978). Examples include the Kobayashi (Kobayashi 1976, 1984) and the Carathéodory distances (Vesentini 1983; Earle et al. 2003).

Keeping within the context of ABC and its applications within engineering, the following distance functions will be reviewed in the section and deployed in the subsequent studies: (1) the Euclidean distance d_E; (2) the Bhattacharyya distance d_B; (3) the Bray–Curtis distance d_{BC}; and (4) the 1-Wasserstein distance d_{W_1}.

Euclidean Distance

The simplest and most commonly implemented distance function to quantify the dissimilarity between the distributions of $\boldsymbol{D}_{\text{sim}}$ and that of the data $\boldsymbol{D}$ is the Euclidean distance function (Khodaparast and Mottershead 2008). Mathematically, it is obtained by calculating the absolute distance between their respective means, which corresponds to the length of the line segment between the means in the Euclidean space (Smith 2013)

$$d_E(\boldsymbol{D}_{\text{sim}}, \boldsymbol{D}) = \sqrt{(\overline{\boldsymbol{D}}_{\text{sim}} - \overline{\boldsymbol{D}})(\overline{\boldsymbol{D}}_{\text{sim}} - \overline{\boldsymbol{D}})^T} \tag{7}$$

where $\overline{\boldsymbol{D}}_{\text{sim}}$ is the row vector of the means associated with the features of $\boldsymbol{D}_{\text{sim}}$; and $\overline{\boldsymbol{D}}$ is the row vector of the means associated with the features of $\boldsymbol{D}$. As such, Eq. (7) simply reflects the point-to-point distance measure between the first-order moment centroids.

Currently, the Euclidean distance function has been implemented within the ABC framework to: (1) provide an initial update on the inferred parameters as part of a two-step ABC framework for the Bayesian inference of failure probability in braced excavation (He et al. 2019); (2) serve as a measure to optimize the computation cost and the tolerance value associated with the population Monte Carlo method used for ABC to address the inverse heat conduction problem (Zeng et al. 2019); (3) perform a "so-called" likelihood-free Bayesian inference on the model parameters of a gamma process using noisy data (Hazra et al. 2020b); (4) perform an analysis to infer model parameters to estimate the flow-accelerated corrosion rate in a nuclear piping system (Hazra et al. 2020a); and (5) perform the uncertainty calibration on the building energy models (Zhu et al. 2020).

Bhattacharyya Distance

The concept of the Bhattacharyya distance function was first developed by Bhattacharyya (1943), and its implementation within the ABC framework was subsequently proposed by Bi et al. (2019), who proposed that the statistical distance can be quantified using such distance. Mathematically, the Bhattacharyya distance between any two distinct PDFs is obtained by computing the degree of overlap between their respective densities (Bhattacharyya 1943)

$$d_B(\boldsymbol{D}_{\text{sim}}, \boldsymbol{D}) = -\log\left[\int_{\Omega} \sqrt{p_{\text{sim}}(\boldsymbol{x}) \cdot p_{\text{D}}(\boldsymbol{x})} d\boldsymbol{x}\right] \tag{8}$$

where Ω denotes the m-dimensional space and the integration is performed over the entire feature space; $p_{\text{sim}}(\cdot)$ is the PDF associated with $\boldsymbol{D}_{\text{sim}}$; and $p_{\text{D}}(\cdot)$ is the PDF associated with $\boldsymbol{D}$.

The number of data features can be greater than one (i.e., $m > 1$), and the integration operation is to be done on the multivariate joint PDFs. This practice can significantly increase the computational demands in performing the operation defined in Eq. (8), especially if the number of data features becomes high (Bi et al. 2022). In addition, a significantly large number of observed data is required to obtain a converged KDE on the PDFs of $\boldsymbol{D}_{\text{sim}}$ and $\boldsymbol{D}$ (Sheather and Jones 1991), which is usually not possible because in practice, limited amount of observed data is available especially in applications where the experiment procedures are complex or computationally expensive (Bi et al. 2022).

To address such issues, a binning algorithm is proposed by Bi et al. (2022) to evaluate the probability mass functions in the form of an approximated discrete distribution on $\boldsymbol{D}_{\text{sim}}$ and $\boldsymbol{D}$. This algorithm yields the discrete Bhattacharyya distance and is computed as (Bi et al. 2022)

$$d_B(\boldsymbol{D}_{\text{sim}}, \boldsymbol{D}) \approx -\log\left[\sum_{i_m}^{N_{\text{bin}}} \cdots \sum_{i_1}^{N_{\text{bin}}} \sqrt{p_{\text{sim}}(b_{i_1,\ldots,i_m}) \cdot p_{\text{D}}(b_{i_1,\ldots,i_m})}\right] \tag{9}$$

where $p_{\text{sim}}(b_{i_1,\ldots,i_m})$ and $p_{\text{D}}(b_{i_1,\ldots,i_m})$ are the probability mass function values of $\boldsymbol{D}_{\text{sim}}$ and $\boldsymbol{D}$, respectively, computed at bin $b_{i_1,\ldots,i_m}$; and N_{bin} is the bin number which is determined empirically (Bi et al. 2022):

$$N_{\text{bin}} = \left\lceil \frac{\max(N_{\text{sim}}, N_{\text{obs}})}{10} \right\rceil \tag{10}$$

where N_{sim} = number of simulated realizations of $\boldsymbol{D}_{\text{sim}}$ computed; N_{obs} = number of observations of $\boldsymbol{D}$ obtained; and $\lceil \cdot \rceil$ is the ceiling operator. As such, the total number of bins N_{tot} based on Eq. (9) is simply $N_{\text{tot}} = (N_{\text{bin}})^m$.

Currently, the Bhattacharyya distance function has been implemented within the ABC framework to accomplish the following: (1) calibrate the structural parameters within a finite-element model corresponding to a two-story frame structure (Bi et al. 2017); (2) perform Bayesian model updating on a seismic-isolated bridge structure based on simulated seismic response data (Kitahara et al. 2021); (3) perform a distribution-free Bayesian model updating on correlated model parameters of dynamical systems (Kitahara et al. 2022a); (4) perform a non-parametric Bayesian model updating on a black-box dynamical system under polymorphic uncertainty (Kitahara et al. 2022b); and (5) calibrate an uncertainty model of a black-box dynamical system based on limited time-domain response data (Bi et al. 2022, 2023).

Bray–Curtis Distance

The Bray–Curtis distance function was first developed by Bray and Curtis (1957) in ecology when quantifying the difference in the abundance of a species between two different locations as a proportion of the total species abundances across both locations (Ricotta and Podani 2017). Such concept of quantifying the statistical difference was recently translated into the context of ABC in comparing two distinct PDFs in the work by Zhao et al. (2022a, b). Mathematically, the Bray–Curtis distance between any two distinct PDFs is obtained by considering the absolute difference between their respective density values following Zhao et al. (2022a)

$$d_{\mathrm{BC}}(\boldsymbol{D}_{\mathrm{sim}}, \boldsymbol{D}) = \frac{\sum_{i_m}^{N_{\mathrm{bin}}} \cdots \sum_{i_1}^{N_{\mathrm{bin}}} |p_{\mathrm{sim}}(b_{i_1,\ldots,i_m}) - p_{\mathrm{D}}(b_{i_1,\ldots,i_m})|}{\sum_{i_m}^{N_{\mathrm{bin}}} \cdots \sum_{i_1}^{N_{\mathrm{bin}}} (p_{\mathrm{sim}}(b_{i_1,\ldots,i_m}) + p_{\mathrm{D}}(b_{i_1,\ldots,i_m}))} \tag{11}$$

where $p_{\mathrm{sim}}(b_{i_1,\ldots,i_m})$ and $p_{\mathrm{D}}(b_{i_1,\ldots,i_m})$ are the probability mass function values of $\boldsymbol{D}_{\mathrm{sim}}$ and $\boldsymbol{D}$, respectively, computed at bin $b_{i_1,\ldots,i_m}$ with m being the total number of data features; and N_{bin} = total number of bins. Based on Eq. (11), the Bray–Curtis distance takes the values between 0 and 1, thereby making it a normalized measure.

Pursuant to the determination of N_{bin}, it was investigated and highlighted in Zhao et al. (2022a) that the traditional binning algorithm in Eq. (10) may not be optimal for the efficient kernel evaluation to compute the Bray–Curtis distance function. To provide for an optimal value of N_{bin} in a less empirical manner, Zhao et al. (2022a) proposed an adaptive binning algorithm, to which the procedure is as follows. The width parameter for each bin w_{bin} is first computed following

$$w_{\mathrm{bin}} = \frac{\log\{\max[\max|\boldsymbol{D}_{\mathrm{sim},i,j} - \boldsymbol{D}_{\mathrm{sim},k,j}|] + 1\}}{\max(N_{\mathrm{sim}}^{1/3}, N_{\mathrm{obs}}^{1/3})} \cdot \exp[d_E(\boldsymbol{D}_{\mathrm{sim}}, \boldsymbol{D})] \tag{12}$$

where $i, k = 1, \ldots, N_{\mathrm{sim}}$, $j = 1, \ldots, m$, and $d_E(\cdot)$ is the Euclidean distance function [i.e., see Eq. (7)]. From which, the value of N_{bin} is computed (Zhao et al. 2022a)

$$N_{\mathrm{bin}} = \left\lceil \frac{\max[\max|\boldsymbol{D}_{\mathrm{sim},i,j} - \boldsymbol{D}_{\mathrm{sim},k,j}|]}{w_{\mathrm{bin}}} \right\rceil \tag{13}$$

where the resulting value of N_{bin} is such that

$$2 \le N_{\mathrm{bin}} \le \left\lceil \frac{\max(N_{\mathrm{sim}}, N_{\mathrm{obs}})}{10} \right\rceil$$

and the total number of bins N_{tot} is simply $N_{\mathrm{tot}} = (N_{\mathrm{bin}})^m$.

Currently, the Bray–Curtis distance function has been implemented within the ABC framework to (Zhao et al. 2022a, b): (1) infer the Young's modulus and shear modulus parameters of a steel plate structures; (2) infer the stiffness parameters of a three degrees-of-freedom spring-mass system; and (3) calibrate an uncertainty model of a black-box dynamical system based on limited time-domain response data.

1-Wasserstein Distance

The definition of the Wasserstein distance function was first conceptualized by Kantorovich (1939) while developing the mathematical method toward production planning and organization (Kantorovich 1939). However, the term "Wasserstein distance" was never used until 1970 when Dobrushin first coined it after obtaining inspiration from a work by Vaserstein, which investigated the Markov process used to describe large automated systems (Vaserstein 1969). Generally speaking, the distance function stems from the optimal transport problem involving the "transportation" of a mass following a given probability mass function, into another probability mass function, which in this context would be the transformation from p_{sim} to that of p_{D}. Such transportation would incur a cost that needs to be optimized, and the Wasserstein metric corresponds to the solution to the optimal transport cost (Bernton et al. 2019; Nadjahi et al. 2020). Mathematically, the general p-Wasserstein distance considers the statistical difference between any two distinct distributions by considering the width enclosed by their corresponding cumulative density functions (CDFs) (Sun et al. 2022)

$$d_{W_p}(\boldsymbol{D}_{\mathrm{sim}}, \boldsymbol{D}) = \int_{-\infty}^{\infty} (|F_{\mathrm{sim}}(\boldsymbol{x}) - F(\boldsymbol{x})|^p d\boldsymbol{x})^{\frac{1}{p}} \tag{14}$$

where $F_{\mathrm{sim}}(\cdot)$ and $F(\cdot)$ are the CDFs of $\boldsymbol{D}_{\mathrm{sim}}$ and $\boldsymbol{D}$, respectively; and p denotes the moment number. Hence, the 1-Wasserstein distance function is the case where $p = 1$, and it is the area enclosed by the CDFs of $\boldsymbol{D}_{\mathrm{sim}}$ and $\boldsymbol{D}$, about which a mathematical proof is provided in (de Angelis and Gray 2021) in the univariate case or a hyper-volume in the multi-variate case. Based on Eq. (14), the 1-Wasserstein distance function is simplified to (Panaretos and Zemel 2019)

$$d_{W_1}(\boldsymbol{D}_{\mathrm{sim}}, \boldsymbol{D}) = \int_{-\infty}^{\infty} |F_{\mathrm{sim}}(\boldsymbol{x}) - F(\boldsymbol{x})| d\boldsymbol{x} \tag{15}$$

Currently, the 1-Wasserstein distance function has been implemented within the ABC framework to: (1) perform Bayesian model updating on a time-series model describing a first-order autoregressive process (Bernton et al. 2019); (2) calibrate an uncertainty model of a black-box dynamical system based on limited time-domain response data (Gray et al. 2022; Lye et al. 2022c); (3) perform Bayesian model updating on the distribution model of the aleatory reliability parameters based on a sparse data set (Lye et al. 2023b); and (4) perform Bayesian model updating on a fatigue crack growth model (Wang et al. 2023).

Numerical Study

The section presents a simple numerical study with the following two objectives: (1) to demonstrate the implementation of each of the distance functions presented previously; and (2) to assess and evaluate their relative strengths and weakness in quantifying the statistical difference between any two sample sets.

For the numerical study, five distinct sets of samples of size $N =$ 10,000 are considered, which are denoted as $\{x_1, x_2, x_3, x_4, x_5\}$. Each of the above samples follow a normal distribution with the corresponding shape parameters defined in Table 1. As an illustration, the histogram representation of the approximated PDFs as well as the empirical cumulative distribution functions (ECDFs) associated with each sample set is presented in Fig. 1.

Table 1. Details on the normal distribution shape parameters for the respective sample set

Sample	Distribution parameters
x_1	$\mu = 2$, $\sigma = 1$
x_2	$\mu = 8$, $\sigma = 2$
x_3	$\mu = 15$, $\sigma = 3$
x_4	$\mu = 15$, $\sigma = 1$
x_5	$\mu = 25$, $\sigma = 1$

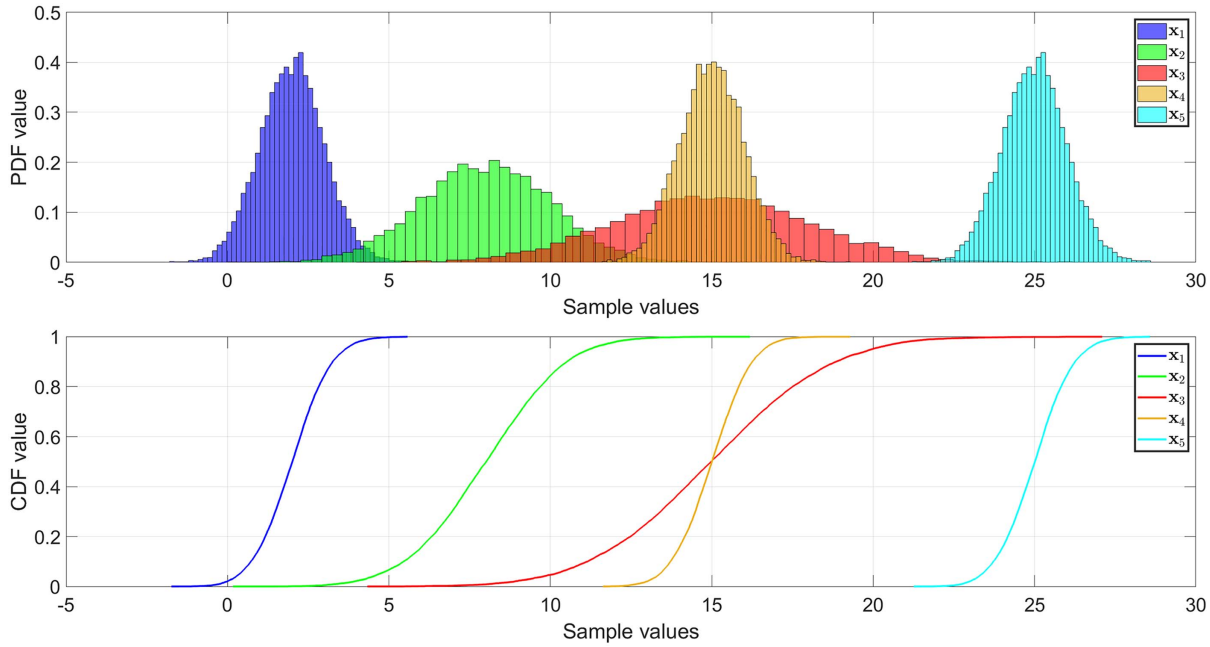

Fig. 1. Histogram representation of the approximated PDFs along with the ECDFs for the respective sample set.

Table 2. Numerical results to the respective distance functions given the corresponding pair of sample sets

Sample set	x_1	x_2	x_3	x_4	x_5
x_1	$d_E = 0$ $d_B = 0$ $d_{\mathrm{BC}} = 0$ $d_{W_1} = 0$	$d_E = 5.99$ $d_B = 2.23$ $d_{\mathrm{BC}} = 0.65$ $d_{W_1} = 5.99$	$d_E = 12.99$ $d_B = 7.23$ $d_{\mathrm{BC}} = 0.78$ $d_{W_1} = 12.99$	$d_E = 13.00$ $d_B = \infty$ $d_{\mathrm{BC}} = 1$ $d_{W_1} = 13.00$	$d_E = 23.00$ $d_B = \infty$ $d_{\mathrm{BC}} = 1$ $d_{W_1} = 23.00$
x_2	$d_E = 5.99$ $d_B = 2.23$ $d_{\mathrm{BC}} = 0.65$ $d_{W_1} = 5.99$	$d_E = 0$ $d_B = 0$ $d_{\mathrm{BC}} = 0$ $d_{W_1} = 0$	$d_E = 6.99$ $d_B = 1.12$ $d_{\mathrm{BC}} = 0.67$ $d_{W_1} = 6.99$	$d_E = 7.00$ $d_B = 3.20$ $d_{\mathrm{BC}} = 0.80$ $d_{W_1} = 7.00$	$d_E = 17.01$ $d_B = \infty$ $d_{\mathrm{BC}} = 1$ $d_{W_1} = 17.01$
x_3	$d_E = 12.99$ $d_B = 7.23$ $d_{\mathrm{BC}} = 0.78$ $d_{W_1} = 12.99$	$d_E = 6.99$ $d_B = 1.12$ $d_{\mathrm{BC}} = 0.67$ $d_{W_1} = 6.99$	$d_E = 0$ $d_B = 0$ $d_{\mathrm{BC}} = 0$ $d_{W_1} = 0$	$d_E = 0.01$ $d_B = 0.29$ $d_{\mathrm{BC}} = 0.49$ $d_{W_1} = 1.61$	$d_E = 10.01$ $d_B = 3.39$ $d_{\mathrm{BC}} = 0.69$ $d_{W_1} = 10.01$
x_4	$d_E = 13.00$ $d_B = \infty$ $d_{\mathrm{BC}} = 1$ $d_{W_1} = 13.00$	$d_E = 7.00$ $d_B = 3.20$ $d_{\mathrm{BC}} = 0.80$ $d_{W_1} = 7.00$	$d_E = 0.01$ $d_B = 0.29$ $d_{\mathrm{BC}} = 0.49$ $d_{W_1} = 1.61$	$d_E = 0$ $d_B = 0$ $d_{\mathrm{BC}} = 0$ $d_{W_1} = 0$	$d_E = 10.00$ $d_B = \infty$ $d_{\mathrm{BC}} = 1$ $d_{W_1} = 10.00$
x_5	$d_E = 23.00$ $d_B = \infty$ $d_{\mathrm{BC}} = 1$ $d_{W_1} = 23.00$	$d_E = 17.01$ $d_B = \infty$ $d_{\mathrm{BC}} = 1$ $d_{W_1} = 17.01$	$d_E = 10.01$ $d_B = 3.39$ $d_{\mathrm{BC}} = 0.69$ $d_{W_1} = 10.01$	$d_E = 10.00$ $d_B = \infty$ $d_{\mathrm{BC}} = 1$ $d_{W_1} = 10.00$	$d_E = 0$ $d_B = 0$ $d_{\mathrm{BC}} = 0$ $d_{W_1} = 0$

For each pair of sample sets, the Euclidean, Bhattacharya, Bray–Curtis, and the 1-Wasserstein distances are computed and the numerical results are presented in Table 2 along with the statistics of the computation time associated with the respective distance function, which is presented in Table 3. From the results presented in Tables 2 and 3, the following evaluation can be made on each of the distance functions.

The Euclidean distance is nonparametric given that there is no requirement to compute any hyperparameters in the form of the number of bins N_{bin}. There are two notable advantages to its implementation: the first is that the Euclidean distance is relatively the most straight-forward distance function in terms of its computation procedure. The second is that, owing to the absence of the need to compute any hyper-parameters, the Euclidean distance function has a relatively low computational requirement. This method results in the distance function having the lowest mean computation time among the four distance functions, as reflected in Table 3. However, a key drawback of the Euclidean distance function is that it only considers the point-to-point distance between the sample means of the two sample sets under consideration and does not account for the difference in their higher-order moments such as their variance (Zhao et al. 2022a, Abdessalem et al. 2019). An example

Table 3. Statistics of the computation time associated with the respective distance function

Distance function	d_E	d_B	d_{BC}	d_{W_1}
Mean $[s]$	1.20×10^{-4}	2.53×10^{-4}	0.90	1.86×10^{-3}
Stdev. $[s]$	9.87×10^{-5}	7.75×10^{-5}	1.82×10^{-2}	1.23×10^{-4}

to illustrate this limitation is found in the result of the Euclidean distance between the pair of sample sets $\{x_3, x_4\}$. The distance value is 0.01 (i.e., close to zero), which implies that the pair of sample sets $\{x_3, x_4\}$ are identically distributed; however, it is their sample means which are similar and not their standard deviations, as reflected in Table 1. Another example would be the case when the pair of sample sets $\{x_1, x_4\}$ are considered, which yields a distance value of 13.00. The result may seem to suggest a significant difference in the statistical distributions between the two sample sets when in fact, the pair of sample sets $\{x_1, x_4\}$ are identically distributed up to their mean values, as reflected in Table 1.

The Bhattacharyya distance is a parametric distance function given the need to compute the parameter N_{bin} to approximate the discrete probability mass function on the sample sets under consideration and compute the overlap between their respective probability mass function [i.e., see Eq. (9)]. There are two advantages to its implementation: the first is that the distance function is "tune-free" because the hyper-parameter N_{bin} is computed automatically using Eq. (10) and there is no need for the user to manually decide its value. The second is that, although the procedure of computing N_{bin} and approximating the discrete probability mass functions may contribute significantly to the computational requirements of the distance function, it can be seen from Table 3 that its mean computation time is still considerably low, which makes the distance function relatively computationally-efficient. However, a key drawback of the Bhattacharyya distance function is that it only accounts for the overlap between the probability mass functions and does not consider the information on the distribution moment of the sample sets under consideration. As such, it is possible to attain an undefined distance value. An example can be found in the result of the Bhattacharyya distance between the pair of sample sets $\{x_1, x_4\}$, where the distance value obtained is infinity. The result may suggest a vast difference in the statistical properties between the two given sample sets when in fact, both sample sets are identically distributed up to their mean values. Such drawback is due to the absence of any degree of overlap between the approximated probability mass functions of x_1 and x_4, which yields a 0 in the argument of the logarithmic operation [i.e., Eq. (9)]. In this instance, the Bhattacharyya distance function becomes inapplicable to quantify the statistical difference between the two given sample sets, which makes the distance function insensitive to the relative center of mass between the two sample sets. To mitigate such drawback, Bi et al. (2019) proposed a two-stage ABC framework that involves performing the first round of ABC procedure using the Euclidean distance function to force an overlap between the probability distributions of the simulated model output and the observed data set before implementing the second round of ABC using the Bhattacharyya distance function.

The Bray–Curtis distance is a relatively recent distance function implemented within the context of ABC (Zhao et al. 2022a, b). Like the Bhattachryya distance, it is parametric distance function because it also requires the computation of N_{bin} to approximate the discrete probability mass function on the sample sets under consideration. There are two advantages to its implementation: The first is that the distance function is "tune-free" because the value of N_{bin} is computed via the adaptive binning algorithm. Such technique provides for a less empirical and a relatively more robust approach toward determining the value of N_{bin} by taking into consideration the effects of the Euclidean distance between the two sample sets and their respective sample sizes [i.e., Eq. (12)]. The second is that, unlike the other distance functions, there exists a hard upper bound on the Bray–Curtis distance value as it is normalized within the interval of $[0, 1]$. This feature is illustrated in the results presented in Table 2. As such, there is no concern over the distance value approaching toward infinity and ensures that the distance function remains applicable in quantifying the statistical difference between any two given sample sets. However, there are two significant drawbacks of the Bray–Curtis distance function. The first is that the Bray–Curtis distance, like the Bhattacharyya distance, accounts only for the degree of overlap between the probability mass functions of the two sample sets. The difference is that the former does so by considering only the absolute difference between their probability mass function values [i.e., Eq. (11)]. This implies that the distance function does not account for the difference in the distribution moment of the sample sets considered and that if there is no overlap between their probability mass functions, the distance function returns the value one. The second drawback is that in the event there is no overlap between the respective probability mass functions of the two sample sets, the Bray–Curtis distance function would always return the value one regardless of how statistically different they are. For example, consider the sample set pairing of $\{x_1, x_4\}$ and $\{x_1, x_5\}$ where in both cases, the distance function returns one regardless of the fact that the center of the probability mass function of x_5 is located further from that of x_1 compared with that of x_4 relative to x_1. In this scenario, the Bray–Curtis distance function fails to reflect the difference in magnitude of the statistical difference between a sample set pairs, which makes the distance function less applicable. Such problem, however, can be mitigated using the same approach proposed by Bi et al. (2019) in dealing with the case when the Bhattachryya distance function yields an undefined value.

Finally, the 1-Wasserstein distance is a non-parametric distance function because there is no need to compute any hyperparameters in the form of N_{bin}. This feature reduces the computation requirement of the distance function which resulted in a considerably short computation time on average as shown in Table 3. A key difference between the 1-Wasserstein distance function and the other distance functions is that it considers the CDFs of the two sample sets considered instead of their PDFs (i.e., in the form of their approximated probability mass functions). There are two notable advantages to its implementation: the first is that by measuring the area enclosed between the respective CDFs, it allows for the statistical difference between the two sample sets to be quantified while also incorporating the information on the distribution moments of the respective sample sets (Sun et al. 2022). The second is that unlike the other distance functions, the 1-Wasserstein distance function can compute the statistical difference between the two given sample sets based on their ECDFs without the need to implement any approximation techniques to estimate their respective analytical CDFs. This eliminates the subjectivity of the distance function to the size of the sample set. However, a significant drawback of the 1-Wasserstein distance function is that its computation can only be done for one component at a time and is unable to do so across multiple dimensions (i.e., $m \geq 2$) simultaneously as per the case of the other three distance functions. This drawback makes the 1-Wasserstein distance function unable to account for the correlation information in quantifying the statistical difference between two given sample sets with multiple components. Such drawback presents an open research question.

Table 4. Details on the respective uncertain input parameters

Parameter	Category	Uncertainty model
p_1	III	Unimodal beta: $3/5 \le E[p_1] \le 4/5$; $1/50 \le V[p_1] \le 1/25$
p_2	II	Interval: $[0, 1]$
p_3	I	Uniform: $[0, 1]$
p_4, p_5	III	Normal: $-5 \le E[p_j] \le 5$; $1/400 \le V[p_j] \le 4$; $\lvert\rho\rvert < 1$ (for $j = 1, 2$)

Note: $E[\cdot]$ is the mean operator, $V[\cdot]$ is the variance operator, and ρ is the correlation coefficient.

Case Study 1: The Nasa-Larc Multidisciplinary UQ Challenge

The set-up presented in the section is adopted from subproblem A of the 2014 NASA-LaRC Multidisciplinary Uncertainty Quantification Challenge (Crespo et al. 2014). The sub-problem is specifically chosen due to its relevance to the scope of the paper. The objectives of this case study are to compare and evaluate: (1) the effectiveness of the uncertainty characterization of the uncertain model parameters under limited information; and (2) the validation performance of a static model given the different distance function implemented toward performing a distribution-based Bayesian model updating via ABC. For this purpose, the focus of the section is on addressing problems A1 and A2 of subproblem A of the challenge.

Problem Description

The set-up involves a black-box subsystem in which scalar output x_1 depends on five uncertain input parameters $p_{1:5}$ via a black-box model following (Crespo et al. 2014)

$$x_1 = h_1(p_1, p_2, p_3, p_4, p_5) \tag{16}$$

Each of the five uncertain input parameters can be classified into one of the following three categories:

- Category I: an aleatory uncertainty which is characterized as a random variable with a fixed functional form and known coefficients. The uncertainty is irreducible;
- Category II: an epistemic uncertainty which is characterized as an unknown but fixed constant which lies within a given interval. The interval is reducible;
- Category III: an aleatory uncertainty modeled as a distributional probability box (p-box) where each parameter prescribing the random variable is an unknown element within a given interval (Ferson et al. 2003) These intervals are reducible.

Details on $p_{1:5}$ are presented in Table 4.

The first part of the problem involves calibrating the uncertainty models of the respective input parameters $p_{1:5}$. To do so, a data set comprising 25 observations of x_1 corresponding to the "true" uncertainty model of each input parameter is provided as the training data. The second part of the problem involves validating the calibrated uncertainty models of the respective input parameters. It will be done through the black-box model h_1 against a set of validation data comprising of another 25 observations of x_1. As an illustration, the ECDF and histogram representations of the training, validation, and the combined (i.e., training and validation) data sets are presented in Fig. 2.

Bayesian Model Updating Set-Up

The calibration of the uncertainty models of the respective input parameters $p_{1:5}$ involves updating the epistemic uncertainties associated with each of the 8 category II parameters: $\boldsymbol{\theta} = \{E[p_1], V[p_1], p_2, E[p_4], V[p_4], E[p_5], V[p_5], \rho\}$. Note that because p_1 is modeled to follow a unimodal beta distribution, which is defined by the shape parameters α and β, it is possible to re-express the shape parameters in terms of $E[p_1]$ and $V[p_1]$ using the method of moments such that

$$\alpha = \left(\frac{E[p_1] \cdot (1 - E[p_1])}{V[p_1]} - 1\right) \cdot E[p_1] \tag{17}$$

$$\beta = \left(\frac{E[p_1] \cdot (1 - E[p_1])}{V[p_1]} - 1\right) \cdot (1 - E[p_1]) \tag{18}$$

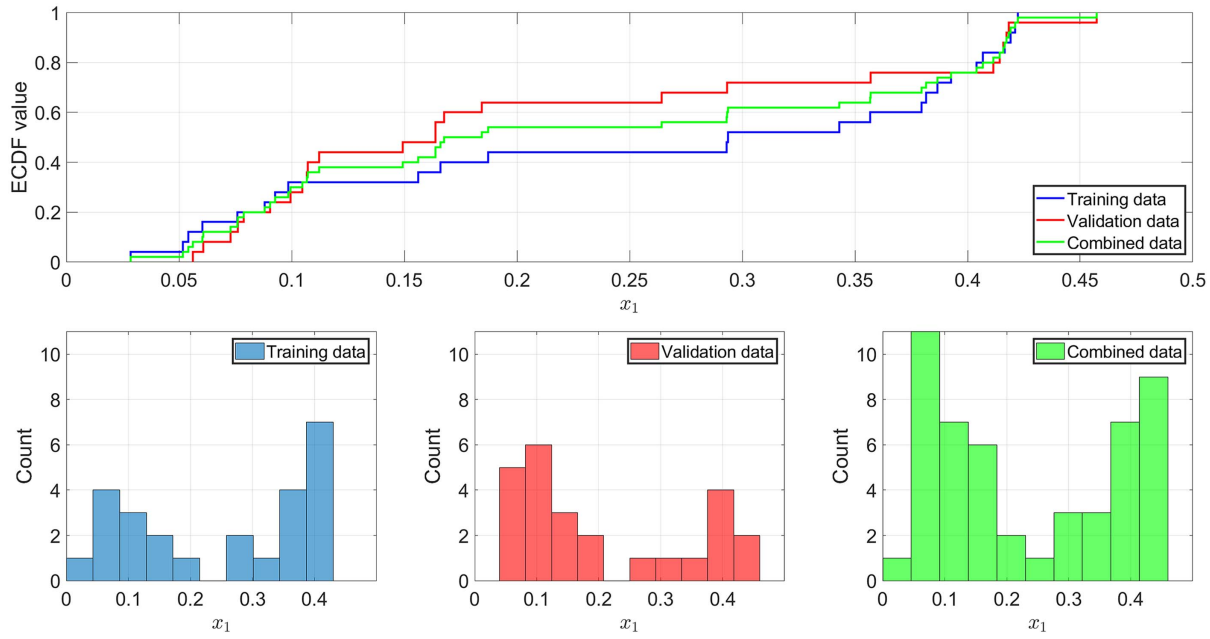

Fig. 2. ECDF and histogram representations of the training, validation, and the combined data sets of x_1.

Table 5. Values of the width factor ε implemented for the respective distance function

Distance function	d_E	d_B	d_{BC}	d_{W_1}
ε	4.0×10^{-3}	3.5×10^{-2}	4.5×10^{-2}	7.0×10^{-3}

to allow the parameters $E[p_1]$ and $V[p_1]$ to be updated directly during the model calibration process.

An approach toward calibrating the uncertainty models of $p_{1:5}$ would be the Bayesian model updating technique. However, such technique becomes inapplicable in reducing the epistemic uncertainty when such uncertainty is represented by intervals, as in this case. To overcome this issue, the intervals describing the uncertainty over the epistemic parameters can be modeled as uniform distributions. By doing so, the prior distribution is defined and samples can be obtained from such intervals. Such approach has been implemented in (Patelli et al. 2015; Bi et al. 2019; Lye et al. 2022c). At this point, note that the subsequent posterior distribution can be interpreted as the fuzzy sets where different levels of statistical significance $L_c \in [0, 1]$ (i.e., alpha-cut level) would yield the updated intervals of varying width because the Bayesian model updating approach seeks to update the epistemic intervals of the corresponding category II parameters rather than providing a probability distribution (i.e., the posterior distribution) over the intervals. Such interpretation was proposed in (Dubois and Prade 1988; Dubois et al. 2004) and implemented in (Beer et al. 2013; Patelli et al. 2015; Lye et al. 2022c).

Based on the justification provided, the prior distribution on $\boldsymbol{\theta}$ can be set as a multivariate (i.e., 8-dimensional) uniform distribution where the bounds for each component of $\boldsymbol{\theta}$ are defined by the corresponding epistemic bounds listed in Table 4. It will be assumed in the problem that the components of $\boldsymbol{\theta}$ are independent from one another. The likelihood function is set as the approximate Gaussian likelihood function defined in Eq. (6). For the problem, the concept of "sufficient" convergence on the resulting posterior distribution is that which requires 10 sampling iterations by the TEMCMC sampler. To achieve this condition, the width factor ε for the respective distance function is set as the following value presented in Table 5. To ensure sufficient degree of sensitivity on (1) the distribution of $\boldsymbol{D}_{\mathrm{sim}}$ relative to that of the training data and (2) the resulting value of the distance function d given each realization of $\boldsymbol{\theta}$, the number of simulated realizations from the black-box model h_1 is set as $N_{\mathrm{sim}} = 30$. The total sample size to be obtained from the resulting posterior distribution is $N = 1{,}000$.

Results and Discussions

The resulting posterior distribution obtained for each component of $\boldsymbol{\theta}$ given the respective distance function is converted into a PDF using the KDE method with a Gaussian kernel from its histogram described with $N_{\mathrm{bin}} = 10$ bins for sufficient resolution of the distribution shape profile. The PDF obtained is normalized such that the peak value corresponds to one to obtain the equivalent fuzzy set for the particular component of $\boldsymbol{\theta}$. The resulting normalized PDFs for each of the 8 category II parameters, given the respective distance function implemented in the Bayesian model updating procedure, are presented in Fig. 3.

From the figure, note that other than the case for $E[p_1]$ and p_2, there is generally no unique solution between the four different distance functions for the remaining 6 category II parameters. In addition, most of the resulting normalized PDFs have multiple peaks.

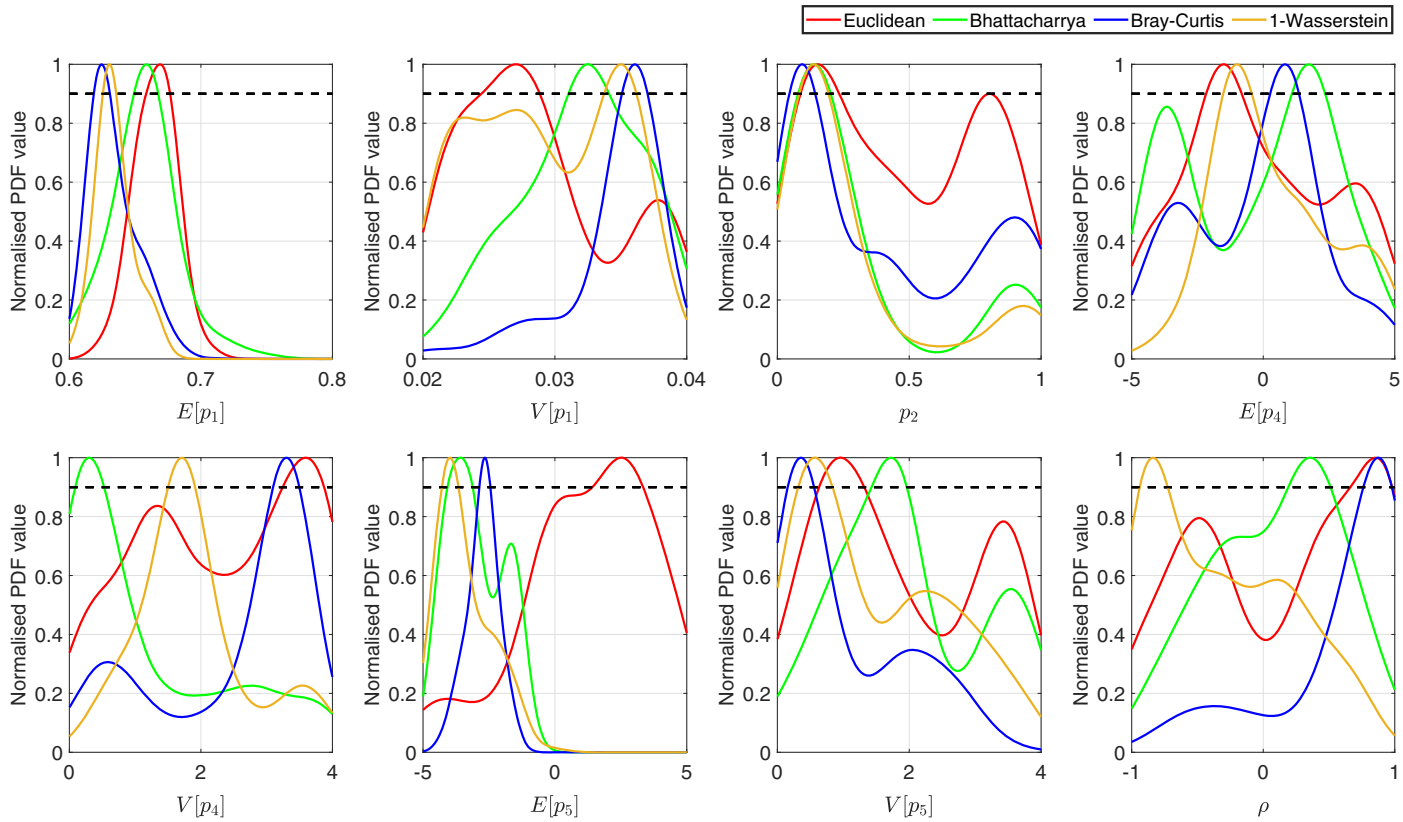

Fig. 3. Normalized PDFs obtained for each inferred parameter given the respective distance function. The black dotted line denotes the alpha-cut level at $L_\alpha = 0.9$.

Table 6. Updated interval of the epistemic uncertainty for the respective inferred parameters obtained at 0.9-level alpha-cut along with the sampling time for each given distance function

Parameter	d_E	d_B	d_{BC}	d_{W_1}
$E[p_1]$	[0.658, 0.677]	[0.649, 0.668]	[0.618, 0.631]	[0.626, 0.636]
$V[p_1]$	[0.024, 0.029]	[0.031, 0.034]	[0.035, 0.037]	[0.034, 0.036]
p_2	[0.088, 0.234]	[0.078, 0.202]	[0.046, 0.144]	[0.082, 0.194]
$E[p_4]$	[−2.174, −0.812]	[1.092, 2.355]	[0.271, 1.373]	[−1.513, −0.431]
$V[p_4]$	[3.239, 3.872]	[0.091, 0.531]	[3.095, 3.495]	[1.501, 1.909]
$E[p_5]$	[1.413, 3.336]	[−4.078, −3.116]	[−2.856, −2.455]	[−4.299, −3.657]
$V[p_5]$	[0.635, 1.312]	[1.429, 1.965]	[0.155, 0.555]	[0.315, 0.836]
ρ	[0.663, 0.980]	[0.190, 0.511]	[0.760, 0.975]	[−0.940, −0.728]
Time (s)	14.54	14.81	15.48	24.67

There are two key reasons to account for the above observations (Bi et al. 2019): (1) the black-box model h_1 takes in multiple model inputs and returns a single scalar model output. This result leads to the case where there are multiple possible solutions to the category II parameters accounted in $\boldsymbol{\theta}$, which may return the same scalar model output (Bi et al. 2019); and (2) the distribution of the training data is bimodal, as illustrated by its histogram in Fig. 2. In fact, the bimodal distribution profile is also observed for the validation data and the combined data, which presents significant evidence that the bimodal distribution profile is an inherent property of the stochastic model output of h_1.

From the fuzzy sets described by the normalized PDFs, a risk-based decision must be made on the updated epistemic intervals for the 8 category II parameters. To provide nonconservative estimates and to ensure that the resulting bounds are obtained only from one of the peaks in the case where the normalized PDF has multiple-peaks, the resulting updated interval for each component of $\boldsymbol{\theta}$ is obtained at an alpha-cut level of $L_\alpha = 0.9$. The resulting updated intervals for each of the category II parameters obtained through the Bayesian model updating approach given the respective distance functions, along with the corresponding sampling time elapsed, are presented in Table 6. Based on the table, the epistemic interval for each of the inferred parameter is generally the tightest in the case of the Bray–Curtis distance compared with the other three distance functions. Such observation is supported by Fig. 3, where the posteriors obtained using ABC via the Bray–Curtis distance have relatively sharp main (i.e., the highest) peaks.

Based on the results presented in Table 6, a p-box on the stochastic model output of h_1 is produced given each distance function using a double-loop Monte Carlo procedure described as follows (Lye et al. 2022c, Rocchetta et al. 2018b): from the updated intervals for the corresponding category II parameters, an 8-dimensional hyperrectangle is defined given each distance function. From the resulting hyper-rectangle, a set of $N_e = 500$ samples are obtained to ensure sufficient exploration of the epistemic space. Each of the N_e epistemic samples is subsequently used as inputs to the uncertainty models for $p_{1:5}$ which, in turn, serve as inputs to h_1. From there, a set of $N_a = 500$ samples of the stochastic model output from h_1 is obtained to ensure sufficient convergence on the distribution describing the aleatory variability on the model output. This output yields N_e distinct ECDFs constructed with N_a stochastic model outputs from which the p-box is obtained (Ferson et al. 2003). The resulting p-box on the stochastic model outputs for the respective distance function implemented in the Bayesian model updating procedure are illustrated in Fig. 4. Based on the figure, note that the resulting p-boxes generally capture the ECDFs of the training and the combined data sets to a large extent. Observe that the p-boxes obtained fail to contain, to a significant extent, the ECDF of the validation data. There are two possible reasons for this finding: (1) a relatively small data size of 25 is used to train and calibrate the uncertainty models for $p_{1:5}$ leading to a poor generalization on the distributions of all possible model outputs; and (2) the distribution profile of the ECDF is sensitive to the sample data provided when the sample size is small. As such, even if the p-box is able to contain the ECDF of the training data, it may fail to contain much of the ECDF of the validation data even though both sets of data are obtained under the same configurations of the uncertainty models for $p_{1:5}$ as inputs to h_1. However, when the combined data is considered, its ECDF is largely contained within the resulting p-box for all the distance functions considered, which provides significant evidence that the Bayesian model updating procedure and the subsequent risk-based decision on the updated epistemic space for the 8 category II parameters considered is sufficiently robust and justified.

To quantify the convergence performance on the stochastic model output given each distance function implemented in the Bayesian model updating procedure, the area of the respective p-box is computed using Eq. (15), to which the results given the respective distance function are presented in Table 7. Based on the table, the implementation of the Euclidean distance function yields the p-box with the tightest width and therefore a relatively higher degree of precision on the distribution of the stochastic model output of h_1 compared with the remaining three distance functions. Despite such result, note that the p-box obtained through the implementation of the Euclidean distance function fails to enclose any of the ECDFs in the lower 30th percentile region, which could be attributed to the fact that the distance function fails to account for the discrepancy in the information pertaining to the higher-order moments of the simulated data $\boldsymbol{D}_{\text{sim}}$ distribution relative to that of the training data during the Bayesian model updating procedure.

To quantify the verification performance on the training data by the $N_a \times N_e$ stochastic model outputs by the respective distance function used in the Bayesian model updating procedure, the discrepancy between each of the N_e model output ECDFs and the ECDF of the training data is quantified by considering the area enclosed between the two ECDFs and computed using Eq. (15) (Ferson et al. 2008). The smaller the area, the smaller the discrepancy between the two ECDFs. Such procedure yields N_e values on the area of the enclosure, from which the mean and standard deviation are obtained. The same procedure is implemented to quantify the validation performance on the validation and the combined data sets. The resulting statistics are presented in Table 8. The mean value of the area obtained is the smallest, in the case of the 1-Wasserstein distance function when the verification performance is considered. This finding can be attributed to the relative strength and capability of the distance function in accounting for the difference in the distribution moments between those of $\boldsymbol{D}_{\text{sim}}$

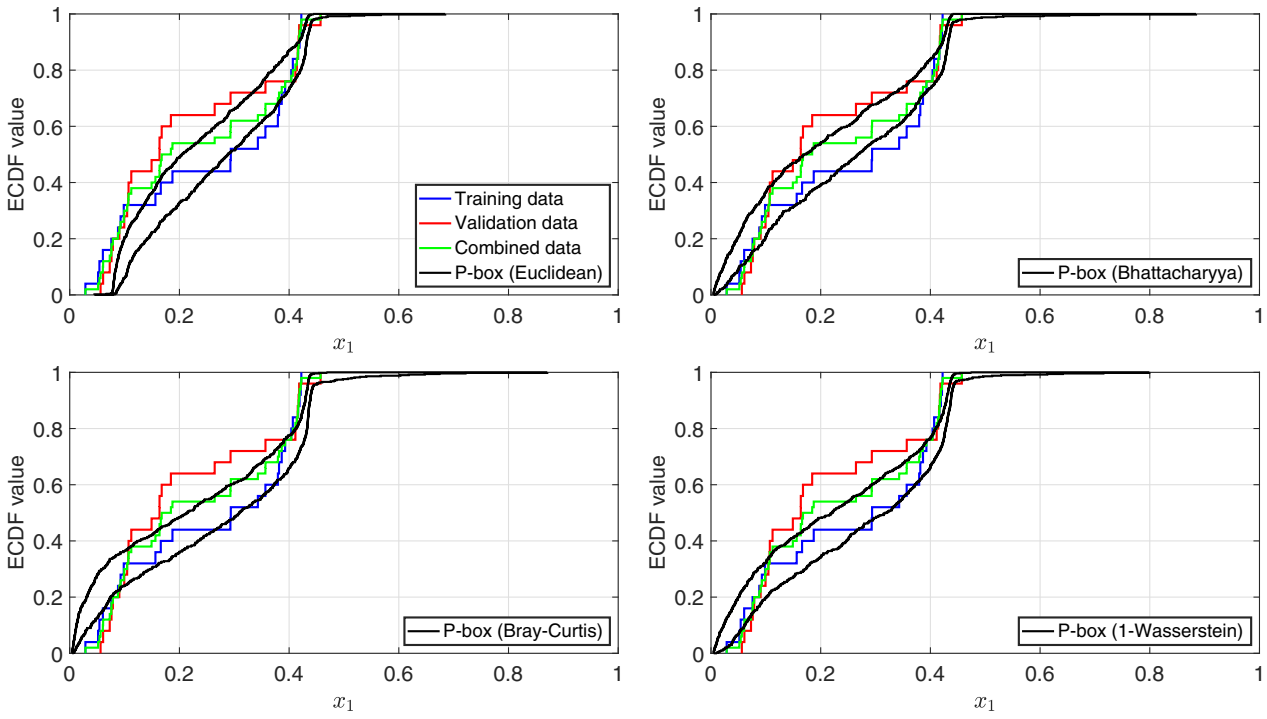

Fig. 4. Resulting p-box obtained from the black-box model h_1 with the calibrated model inputs based the respective distance function implemented in the Bayesian model updating procedure.

Table 7. Results to the area of the p-boxes obtained from h_1 given the respective distance function implemented in the Bayesian model updating procedure

Distance function	d_E	d_B	d_{BC}	d_{W_1}
P-box area	5.17×10^{-2}	5.82×10^{-2}	5.77×10^{-2}	5.66×10^{-2}

distribution and that of the training data during the Bayesian model updating procedure. However, when considering the validation performance, both on the validation and the combined data sets, the mean value of the area obtained is the smallest in the case of the Bhattachryya distance function. This result is supported by the fact that the corresponding p-box of the stochastic model output largely encloses the ECDF of the validation and the combined data sets, as illustrated in Fig. 4, and that the area of the enclosure by the p-box is the largest among the four distance functions considered, as shown in Table 7.

Case Study 2: The Thermal Problem

The set-up presented in the section is adopted from the model validation challenge problem as part of the 2018 Validation Challenge Workshop hosted by the Sandia National Laboratories (Hills et al. 2008). Details of the challenge problem can be found in Dowding et al. (2008). The objectives of this case study are to compare and evaluate the following: (1) the effectiveness of the uncertainty characterization of the aleatory model parameters under limited information; and (2) the validation performance of a dynamical (i.e., time-dependent) model given the different distance function implemented toward performing a Bayesian model updating via ABC.

Problem Description

The set-up involves a slab material that can be used as a component of a nuclear reactor vessel containment structure. The thermal property of the slab material is such that its temperature response T under heating conditions can be mathematically modeled using M_T defined as (Dowding et al. 2008)

$$M_T(x,t) = \begin{cases} T_i, & \text{for } t = 0 \text{ s} \\ T_i + \dfrac{qL}{k}\left[\dfrac{(k/\rho C_p)t}{L^2} + \dfrac{1}{3} - \dfrac{x}{L} + \dfrac{1}{2}\left(\dfrac{x}{L}\right)^2 - \dfrac{2}{\pi^2}\displaystyle\sum_{n=1}^{6}\dfrac{1}{n^2}\exp\left(-n^2\pi^2\dfrac{(k/\rho C_p)t}{L^2}\right)\cos\left(n\pi\dfrac{x}{L}\right)\right], & \text{for } t > 0 \text{ s} \end{cases} \tag{19}$$

where L = thickness of the slab material; x = location variable along the thickness of the slab; t = time since the start of the heating process; T_i = initial ambient temperature; q = heat flux; k = thermal conductivity of the slab material; and ρC_p = heat capacity of the slab material.

The material thermal properties k and ρC_p are set as the aleatory variables. As such, the first part of the challenge is to characterize the aleatory uncertainty over k and ρC_p based on a set of 20 experimental data provided for each thermal property across five different temperature response values: $T = \{20°\mathrm{C}, 250°\mathrm{C}, 500°\mathrm{C},$

Table 8. Results to the corresponding performances by the stochastic model output of h_1 given the respective distance function implemented in the Bayesian model updating procedure

Distance function	Verification		Validation		Validation (combined)	
	Mean	Stdev.	Mean	Stdev.	Mean	Stdev.
d_E	3.45×10^{-2}	3.03×10^{-3}	5.13×10^{-2}	6.78×10^{-3}	3.33×10^{-2}	4.20×10^{-3}
d_B	3.03×10^{-2}	6.35×10^{-3}	4.02×10^{-2}	5.33×10^{-3}	2.03×10^{-2}	2.15×10^{-3}
d_{BC}	2.60×10^{-2}	4.12×10^{-3}	5.89×10^{-2}	6.10×10^{-3}	3.24×10^{-2}	5.85×10^{-3}
d_{W_1}	2.09×10^{-2}	2.80×10^{-3}	5.50×10^{-2}	5.46×10^{-3}	2.86×10^{-2}	5.32×10^{-3}

Table 9. Numerical data for each material property given each value of T

T (°C)	20	250	500	750	1,000
$k(T)$	0.0496	0.0628	0.0602	0.0657	0.0631
	0.0530	0.0620	0.0546	0.0713	0.0796
(W/m°C)	0.0493	0.0537	0.0628	0.0694	0.0692
	0.0455	0.0561	0.0614	0.0732	0.0739
$\rho C_p(T)$	3.76×10^5	3.87×10^5	4.52×10^5	4.68×10^5	4.19×10^5
	3.38×10^5	4.69×10^5	4.10×10^5	4.24×10^5	4.38×10^5
(J/m^3°C)	3.50×10^5	4.19×10^5	4.02×10^5	3.72×10^5	3.45×10^5
	4.13×10^5	4.28×10^5	3.94×10^5	3.46×10^5	3.95×10^5

750°C, 1,000°C}. The corresponding numerical data for each material property is presented in Table 9.

When characterizing the aleatory uncertainty over k and ρC_p, the challenge makes the following three assumptions (Dowding et al. 2008): (1) the diagnostic variability or uncertainty is negligible compared with specimen-to-specimen variability; (2) the estimates of thermal conductivity and that of the volumetric heat capacity are independent between one another; and (3) the estimates of thermal conductivity and that of the volumetric heat capacity are temperature independent.

From which, the second part of the challenge involves performing an ensemble validation of the model predictions by M_T, based on the determined aleatory characterization of k and ρC_p, over a database of experiment data of T obtained from location $x = 0$ cm. The database comprises data across four different experiments, in which each experiment yields 11 experimental data of T of the slab obtained across 11 values of time t between 0 s and 1,000 s at an interval of $\Delta t = 100$ s. The corresponding graphical plot of the validation ensemble data set is presented in Fig. 5, whereas its numerical values are presented in Table 10.

Bayesian Model Updating Set-Up

In characterizing the aleatory uncertainty over k and ρC_p, the challenge did not specify any particular class of distribution for either variable. Based on the ECDF of k and ρC_p presented in Fig. 6, it can be inferred that the distribution profile of both variables is unimodal. Based on the previous work in (Ferson et al. 2008),

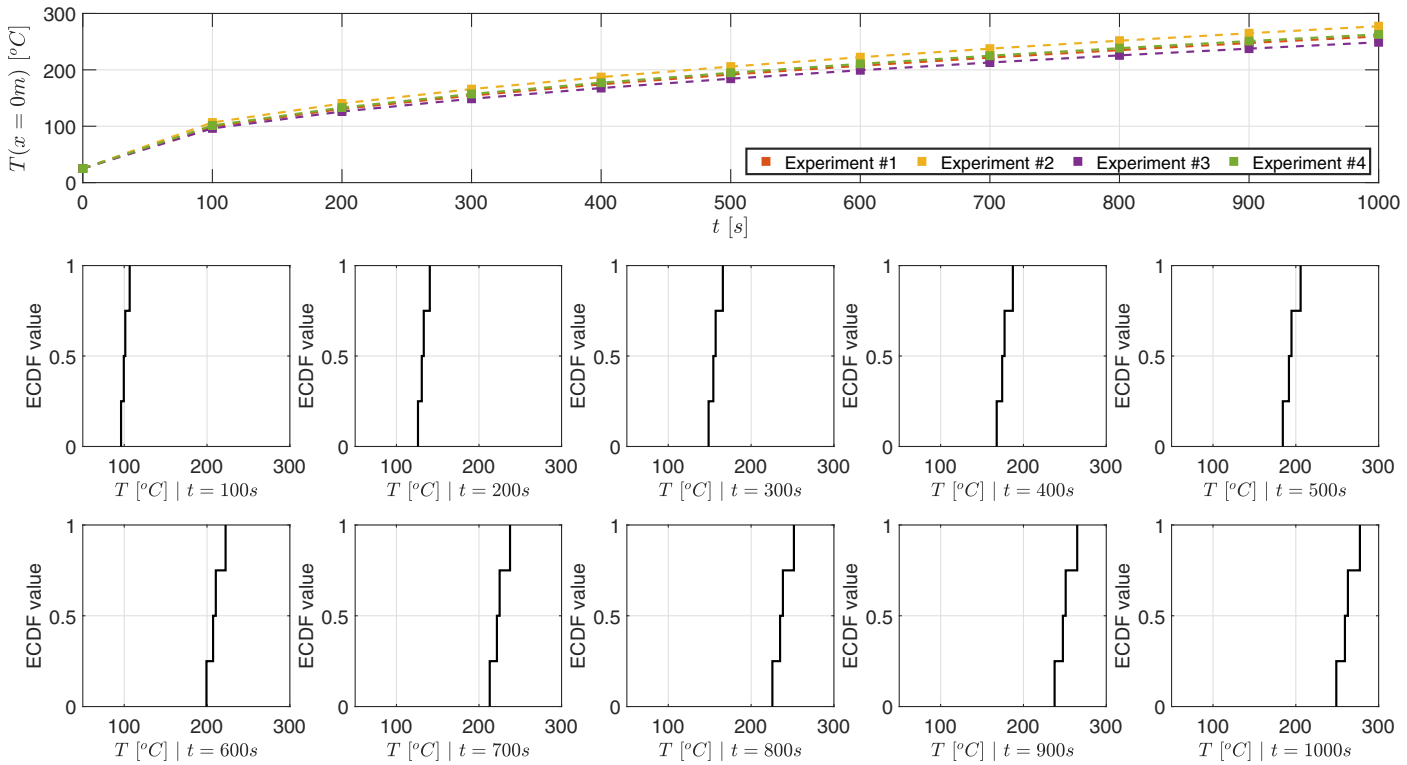

Fig. 5. Graphical plot representation of the validation ensemble data set along with the ECDF of the data across the four experiments at each t.

Table 10. The ensemble validation data set for the model validation of M_T given $q = 1{,}000$ W/m^2 and $L = 2.54$ m

	T (°C)			
t (s)	Exp. #1	Exp. #2	Exp. #3	Exp. #4
0	25.0	25.0	25.0	25.0
100	99.5	106.6	96.2	101.3
200	130.7	140.4	126.1	133.1
300	154.4	165.9	148.7	157.2
400	174.3	187.2	167.7	177.2
500	191.7	205.8	184.3	194.8
600	207.3	222.4	199.3	210.6
700	221.7	237.6	213.0	225.0
800	235.0	251.7	225.7	238.4
900	247.6	264.9	237.6	251.0
1,000	259.5	277.4	248.9	262.9

an appropriate choice of distribution model for both k and ρC_p would be the normal distribution. Note that the focus of this problem is in comparing the model calibration performance k, and ρC_p via ABC, and eventually the model ensemble validation performance of M_T, using the different distance functions and not performing a model selection.

For a given distance function, the Bayesian model updating procedure is implemented to update the shape parameters of the normal distribution to model the variability of k and ρC_p using the TEMCMC sampler. The procedure is described as follows: a uniform prior is first assigned to the distribution parameters of a given distribution model to model their associated epistemic uncertainties. The corresponding prior bounds for the respective distribution parameters are provided in Table 11. The likelihood function is set as the approximate Gaussian likelihood function defined in Eq. (6). For the problem, the concept of "sufficient" convergence on the resulting posterior distribution is that which requires 7 sampling iterations by the TEMCMC sampler. To achieve this outcome, the width factor ε for the respective distance function and distribution model is set as the following value presented in Table 12. To ensure sufficient degree of sensitivity on (1) the distribution of $\boldsymbol{D}_{\text{sim}}$ relative to that of the training data and (2) the resulting value of the distance function d given each realization of $\boldsymbol{\theta}$ (i.e., the shape parameter values of a given distribution model), the number of simulated realizations from the given distribution model is set as $N_{\text{sim}} = 30$. The total sample size to be obtained from the resulting posterior distribution is $N = 1{,}000$.

Table 11. Details on the respective inferred distribution parameters and the corresponding prior bounds

Shape parameter	Description	Prior bounds	Units
μ_k	Mean of k	$[0.02, 0.08]$	(W/m°C)
σ_k	Standard deviation of k	$[0.001, 0.100]$	(W/m°C)
$\mu_{\rho C_p}$	Mean of ρC_p	$[2.00 \times 10^5, 8.00 \times 10^5]$	(J/m^3°C)
$\sigma_{\rho C_p}$	Standard deviation of ρC_p	$[1.00 \times 10^4, 8.00 \times 10^4]$	(J/m^3°C)

Table 12. Values of the width factor ε implemented for the respective distance function

Aleatory parameter	d_E	d_B	d_{BC}	d_{W_1}
k	1.0×10^{-3}	0.06	0.06	1.5×10^{-3}
ρC_p	2.5×10^3	7.0×10^{-2}	3.6×10^{-2}	4.0×10^3

Results and Discussions

Following the approach described in the section "Case Study 1: The Nasa-Larc Multidisciplinary UQ Challenge," the fuzzy sets on the inferred parameters are obtained and are illustrated in Fig. 7. From these fuzzy sets, the resulting updated epistemic intervals on the inferred distribution parameters are obtained at an alpha-cut level of $L_\alpha = 0.9$. The numerical results to the updated intervals for each of the inferred distribution parameters along with the total sampling time elapsed for each given distance function are presented in Table 13.

Based on the results provided in the table, the resulting p-boxes for k and ρC_p obtained via ABC through the respective distance functions are presented in Fig. 8. The p-box for k and ρC_p obtained via ABC using the 1-Wasserstein distance function has the smallest area compared with the Euclidean, Bhattacharyya, and the Bray–Curtis distance functions. Such observation is supported by the

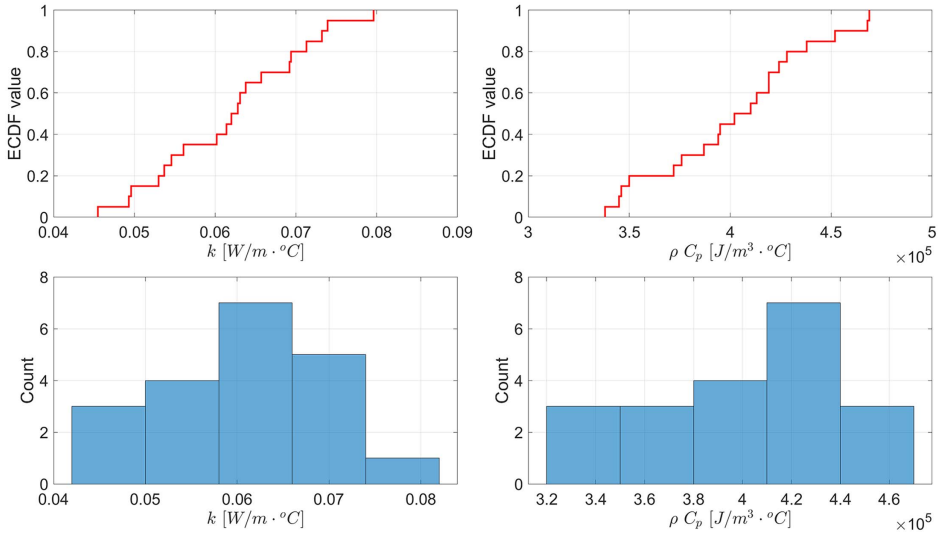

Fig. 6. ECDF and histogram representation of the experimental data for k and ρC_p.

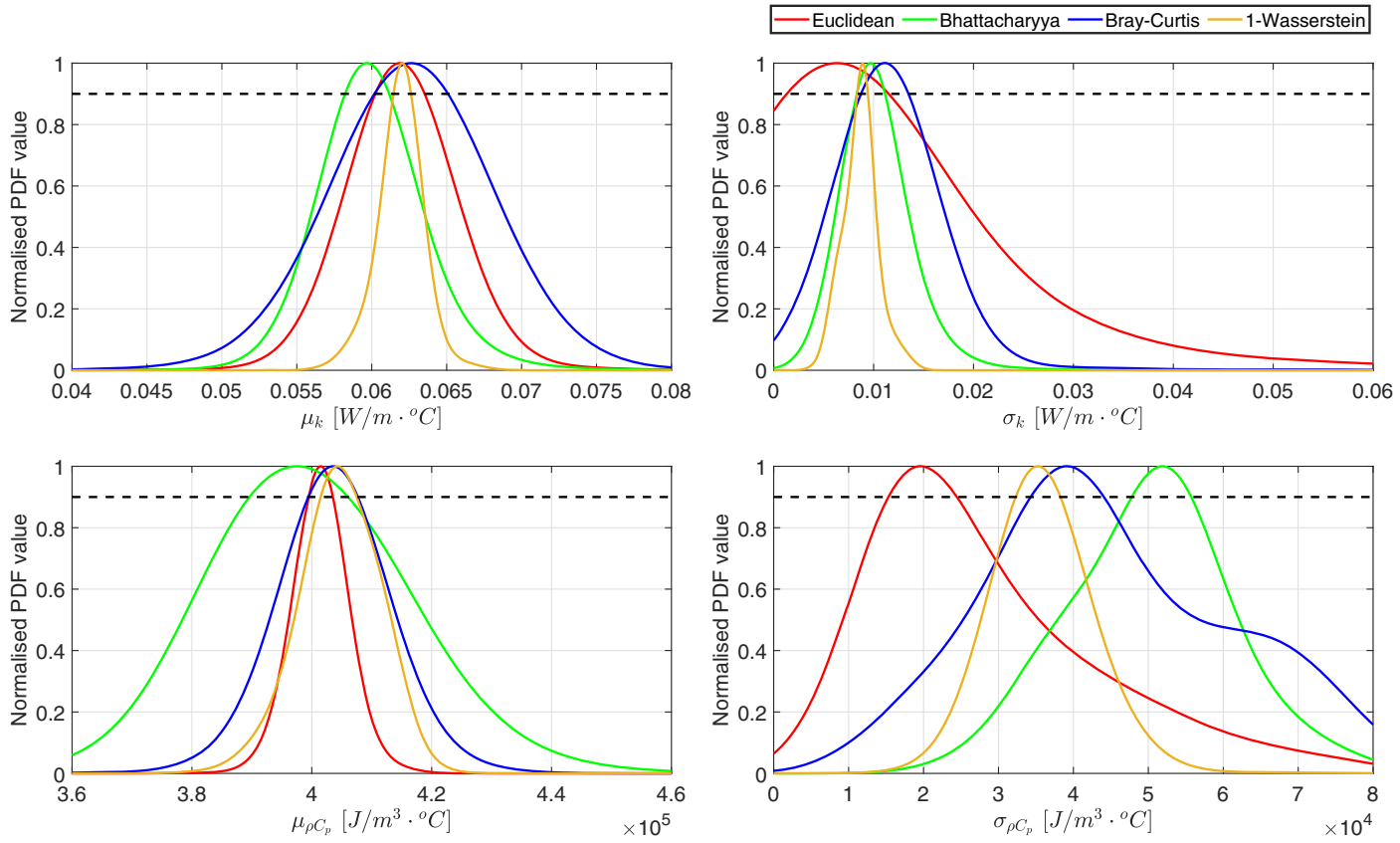

Fig. 7. Normalized PDFs obtained for each inferred parameter given the respective distance function. The black dotted line denotes the alpha-cut level at $L_\alpha = 0.9$.

Table 13. Updated interval of the epistemic uncertainty for the respective inferred parameters obtained at 0.9-level alpha-cut along with the sampling time for each given distance function

Parameter	d_E	d_B	d_{BC}	d_{W_1}
μ_k	$[6.03 \times 10^{-2}, 6.35 \times 10^{-2}]$	$[5.82 \times 10^{-2}, 6.11 \times 10^{-2}]$	$[6.02 \times 10^{-2}, 6.50 \times 10^{-2}]$	$[6.15 \times 10^{-2}, 6.26 \times 10^{-2}]$
σ_k	$[1.32 \times 10^{-3}, 1.15 \times 10^{-2}]$	$[8.30 \times 10^{-3}, 1.12 \times 10^{-2}]$	$[8.78 \times 10^{-3}, 1.35 \times 10^{-2}]$	$[8.42 \times 10^{-3}, 9.38 \times 10^{-3}]$
Time (s) (k)	0.53	0.55	0.71	1.92
$mu_{\rho C_p}$	$[3.99 \times 10^5, 4.03 \times 10^5]$	$[3.89 \times 10^5, 4.06 \times 10^5]$	$[3.99 \times 10^5, 4.08 \times 10^5]$	$[4.01 \times 10^5, 4.07 \times 10^5]$
$\sigma_{\rho C_p}$	$[1.54 \times 10^4, 2.44 \times 10^4]$	$[4.78 \times 10^4, 5.56 \times 10^4]$	$[3.45 \times 10^4, 4.41 \times 10^4]$	$[3.24 \times 10^4, 3.83 \times 10^4]$
Time (s) (ρC_p)	0.44	0.65	0.88	1.82

numerical results presented in Table 14. This finding highlights the advantage of the 1-Wasserstein distance function in its capability to account for the difference in the distribution moments of the data ECDF and the assigned distribution model during the ABC procedure as highlighted in the section "1-Wasserstein Distance," yielding a more precise estimate on the distribution of the aleatory variables. In addition, note in Fig. 8 that the p-box for k and ρC_p obtained via ABC using the Euclidean distance function has a significantly smaller width at the ECDF value of 0.5. This finding is attributed to the fact that the Euclidean distance function is effective when considering the point-to-point distance between the sample means of the two sample sets and not their higher-order moments such as their variance, a drawback which was highlighted in the section "Euclidean Distance."

For each distance function, based on the resulting p-boxes on k and ρC_p, the following double-loop Monte Carlo procedure is undertaken to perform the ensemble validation of the stochastic model output by M_T against the ensemble validation data set at a given t: first, an epistemic space E is represented by the four-dimensional hyper-rectangle with bounds defined in Table 13 for the corresponding distance function. From the epistemic space E, a total of $N_e = 500$ samples of $\boldsymbol{\theta} = \{\mu_k, \sigma_k, \mu_{\rho C_p}, \sigma_{\rho C_p}\}$ are generated from a multivariate uniform distribution. For each of the N_e epistemic sample realization, which now serves as the input parameters to the normal distribution model for k and ρC_p, a total of $N_a = 500$ aleatory sample realizations of k and ρC_p are obtained. This procedure is done for $t = 100$ s to $t = 1{,}000$ s at intervals of $\Delta t = 100$ s and is repeated for all the distance functions. The resulting p-boxes obtained at each t in relation to the ensemble validation data are presented in Fig. 9.

Next, the area of the corresponding p-box area is evaluated at each t where the validation ensemble data are obtained to quantify the convergence performance on the stochastic model output given each distance function. The results are illustrated graphically in Fig. 10, and the corresponding numerical values are presented in Table 15. Based on the results, it is observed that the p-box area

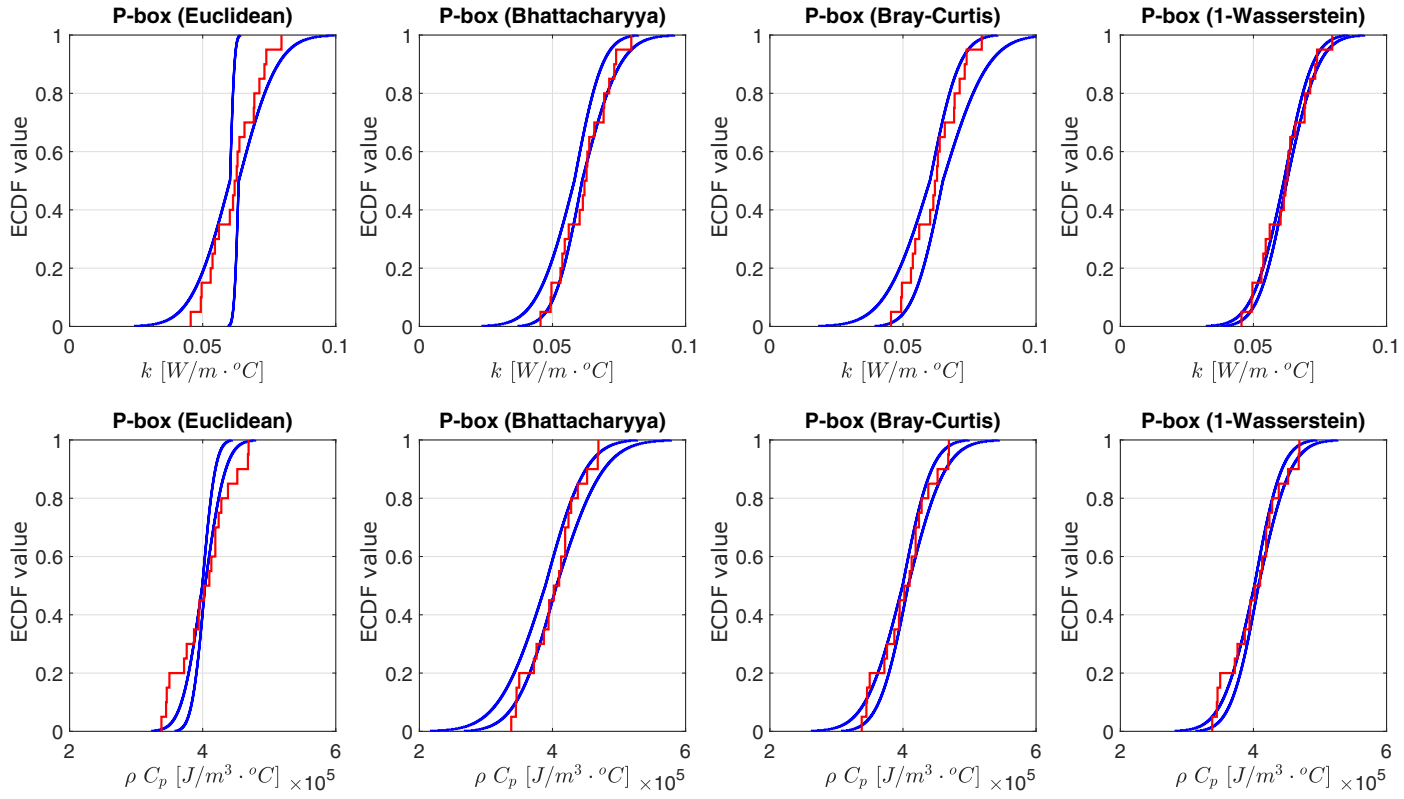

Fig. 8. Resulting p-boxes for k and ρC_p obtained via ABC using the different distance functions.

associated with the use of the Euclidean distance function in the ABC procedure is consistently the lowest across all t, followed closely by those associated with the 1-Wasserstein distance function. This finding highlights the relatively high degree of convergence in the stochastic estimates of the temperatures T that is achieved by the two aforementioned distance functions compared with the Bhattachryya and the Bray–Curtis distance functions.

To quantify the validation performance by the stochastic model M_T on the ensemble validation data given the respective distance function, the procedure follows that described in the section "Case Study 1: The Nasa-Larc Multidisciplinary UQ Challenge." At a given t, for each distance function, the discrepancy between each of the N_e model output ECDFs and the ECDF of the ensemble validation data is quantified by considering the area of enclosure between the two ECDFs and computed using Eq. (15). From there, the statistics in the form of the mean and standard deviation of the area of enclosure are obtained, and these data are presented graphically in Fig. 10 and numerically in Table 16 across all t for the respective distance function. Based on the results, the validation performance by the stochastic model M_T calibrated using the Euclidean distance function generally gives the smallest mean area of enclosure across all t, which indicates the highest degree of agreement between the stochastic model output and the ensemble validation data. Such result is consistent with the observation that the p-box of the stochastic model output is the smallest around the ECDF of the ensemble validation data for all t in the case of the Euclidean distance function. However, when considering the standard deviation of the area of enclosure, the stochastic model M_T calibrated using the 1-Wasserstein distance function generally gives the smallest value across all t, which indicates the highest degree of precision and consistency in the stochastic model output relative to the ensemble validation data.

Table 14. Area of the resulting p-box for k and ρC_p given the respective distance function

Aleatory parameter	d_E	d_B	d_{BC}	d_{W_1}
k (W/m°C)	1.15×10^{-2}	5.30×10^{-3}	8.70×10^{-3}	2.00×10^{-3}
ρC_p (J/m^3°C)	1.14×10^4	2.33×10^4	1.64×10^4	1.12×10^4

Conclusions

The paper has provided an analysis and comparison of the Stochastic model updating performance in approximate Bayesian computation using the following four different distance functions: (1) Euclidean distance between moments; (2) Bhattacharyya distance; (3) Bray–Curtis distance; and (4) 1-Wasserstein distance. It reviewed Bayesian model updating and the motivation behind the need for the distance-based approximate Bayesian computation, followed by a detailed discussion to the distance functions and an exposition of their respective strengths and limitations through a numerical study and the two case studies, which serve as the basis for comparison in the stochastic model updating and model validation performance via approximate Bayesian computation.

For the first case study, a comparison of the uncertainty characterization of the black-box model parameters was undertaken between the four distance measures implemented in the approximate Bayesian computation procedure under limited data. Based on the Bayesian model updating results on the inferred parameters, it was found that the Bray–Curtis distance was able to achieve the tightest bounds on the epistemic interval on each of the inferred parameters at the 0.9 alpha-cut level. A comparison of the model validation performance showed that the Bhattachryya distance provided the

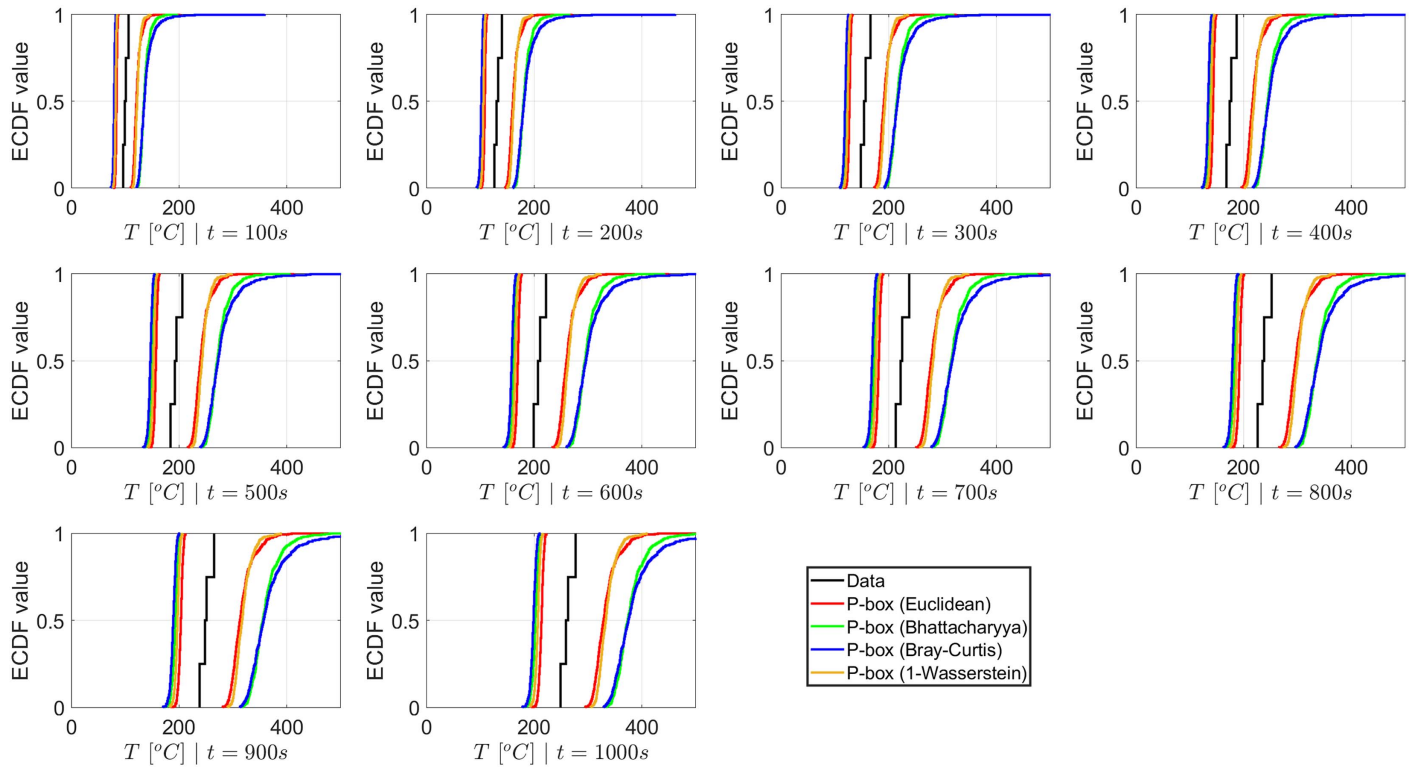

Fig. 9. Resulting p-boxes for the slab temperature T across the given time t. Note that the black ECDF describes the empirical distribution of the ensemble validation data.

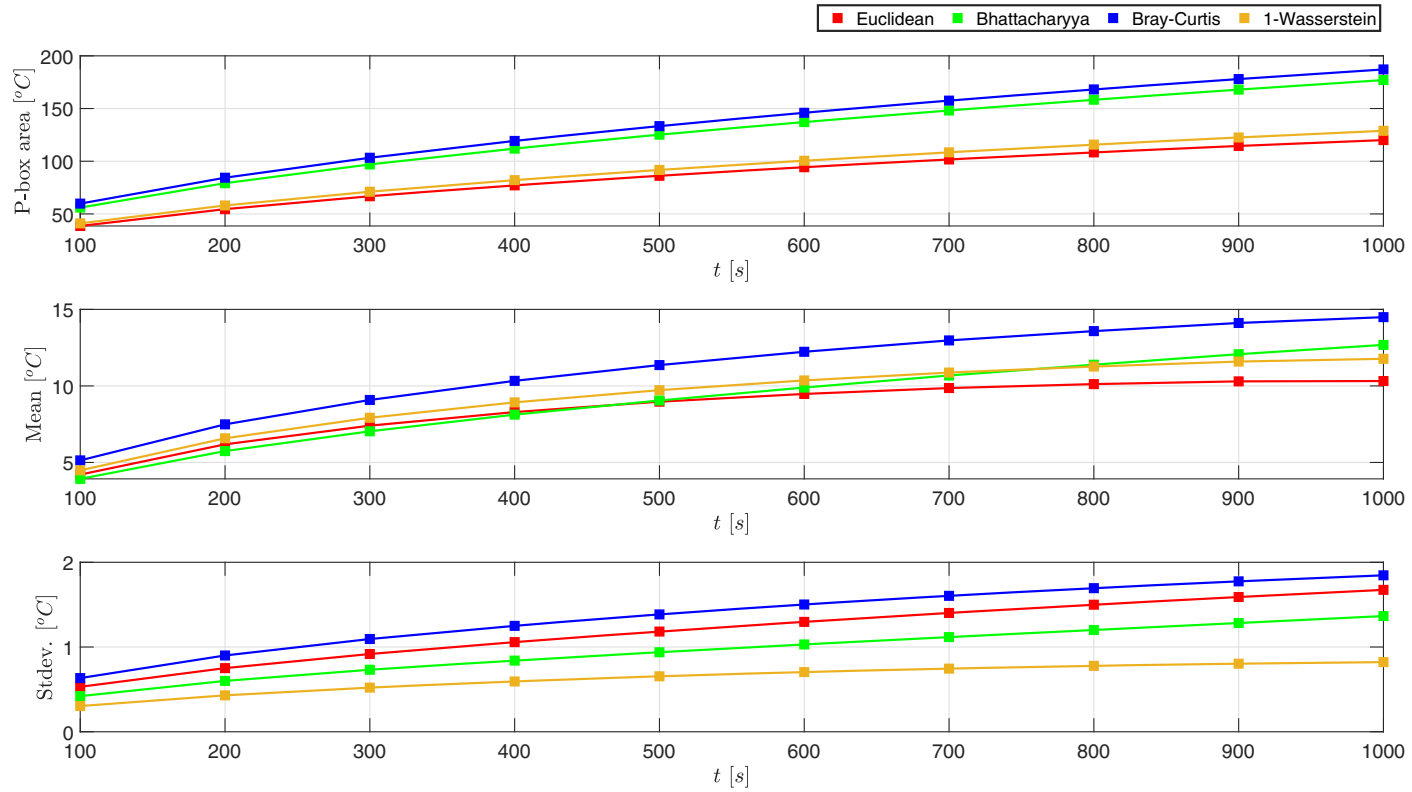

Fig. 10. Resulting graphical plot summarizing the statistics of the validation performance by the model M_T as a result of the updating procedure via ABC using the respective distance functions.

Table 15. The statistics to the p-box area at each t given the respective distance function

t (s)	d_E (°C)	d_B (°C)	d_{BC} (°C)	d_{W_1} (°C)
100	38.93	56.01	53.22	41.04
200	55.04	79.17	74.70	58.03
300	67.41	96.97	91.25	71.07
400	77.83	111.97	105.22	82.07
500	86.98	125.19	117.54	91.74
600	95.19	137.14	128.64	100.46
700	102.63	148.13	138.78	108.42
800	109.39	158.35	148.12	115.76
900	115.56	167.94	156.78	122.55
1,000	121.19	177.02	164.83	128.87

Table 16. The mean statistics to the model validation performance at each t given the respective distance function

t (s)	d_E (°C)	d_B	d_{BC}	d_{W_1} (°C)
100	4.13	3.93	4.52	4.48
	(0.55)	(0.42)	(0.61)	(0.30)
200	6.08	5.74	6.62	6.58
	(0.77)	(0.60)	(0.86)	(0.43)
300	7.28	7.04	8.01	7.92
	(0.95)	(0.73)	(1.05)	(0.52)
400	8.15	8.12	9.09	8.92
	(1.10)	(0.84)	(1.20)	(0.59)
500	8.81	9.05	9.96	9.72
	(1.23)	(0.94)	(1.34)	(0.65)
600	9.31	9.89	10.69	10.36
	(1.36)	(1.03)	(1.46)	(0.70)
700	9.69	10.68	11.30	10.87
	(1.48)	(1.12)	(1.57)	(0.75)
800	9.94	11.39	11.80	11.27
	(1.59)	(1.20)	(1.67)	(0.78)
900	10.11	12.07	12.24	11.59
	(1.69)	(1.28)	(1.75)	(0.80)
1,000	10.13	12.68	12.54	11.77
	(1.78)	(1.37)	(1.83)	(0.82)

Note: Values in brackets are the standard deviation statistics to the model validation performance.

best validation performance compared to the remaining three distance functions.

For the second case study, a comparison of the uncertainty characterization of the aleatory model parameters showed that the 1-Wasserstein distance function provided the tightest bounds on the epistemic interval on each of the inferred parameters at 0.9 alpha-cut level. The resulting p-box obtained for the corresponding aleatory model parameters obtained through the 1-Wasserstein distance function also had the smallest area of enclosure compared with those obtained by the Euclidean, Bhattacharyya, and the Bray–Curtis distance functions. A comparison was made on the model validation performance between the resulting calibrated model between the distance function used, and the Euclidean distance provided the best validation performance, whereas the 1-Wasserstein distance provided the greatest degree of precision and consistency in the stochastic model output relative to the ensemble validation data.

In summary, the paper highlights the following: (1) the strengths and limitations of each distance function in quantifying the statistical difference between a pair of sample distributions; (2) although the 1-Wasserstein distance function seems to be the most robust, in principle, in quantifying the statistical difference between two sample distributions due to its capability in accounting for the difference between their distribution moments, the distance function was unable to provide for the best validation performance by the calibrated stochastic model, as seen in both case studies; (3) the Bhattacharyya distance is noted to provide the best validation performance by the calibrated stochastic black-box model relative to a bimodal validation data set, as seen in the NASA-LaRC Multidisciplinary UQ Challenge; (4) the Euclidean distance, despite seemingly the least robust in quantifying the difference between a pair of sample distributions as highlighted in the section "Review of the Distance Functions," reportedly provides the best validation performance by the calibrated stochastic model relative to an ensemble validation data set, as seen in the thermal problem; and (5) the strength of the 1-Wasserstein distance function was illustrated when characterizing the aleatory variability of the thermal conductivity and the heat capacity parameters of the slab material in the thermal problem when it is observed to yield a probability box with the smallest width.

Through an in-depth review on the four different distance functions, the following points are identified as potential areas for future research work: (1) the current scope of work here considers only for the case where the output space is unidimensional. Further works shall involve case studies where the output space is multidimensional (e.g., 10 dimensions or more) to provide a better assessment on the robustness of the distance functions in stochastic model updating and model validation performances under significantly complex conditions; (2) the proposed adaptive binning algorithm that is implemented in the Bray–Curtis distance function considers the case where there is a relatively large data set (i.e., above 100 data sets) in (Zhao et al. 2022a) and did not account for cases where the data set is small, as per the case studies presented. Further research efforts may be invested toward formulating improved binning strategies to better resolve the distribution of the limited observed data and improve the distance computation for the Bhattacharyya and the Bray–Curtis distance functions. This progression, in turn, seeks to improve the stochastic model updating performance from what is presented in the paper; and (3) the development of a hypervolume metric as an extension to the area metric, along with the formulation of a computationally efficient numerical integration approach to compute the hypervolume in a multidimensional space, especially for 5 dimensions and greater.

To provide a better understanding on the concept of Approximate Bayesian Computation along with the implementation of the different distance functions discussed in the paper, as well as to allow for the reproducibility of the results presented in the paper, the MATLAB codes to the case studies are made available and freely accessible on GitHub (Lye, n.d.).

Data Availability Statement

The authors confirm and declare that the data and the codes that support the findings in the paper are made openly accessible on GitHub (Lye, n.d.).

References

Abdessalem, A. B., N. Dervilis, D. Wagg, and K. Worden. 2019. "Model selection and parameter estimation of dynamical systems using a novel variant of approximate Bayesian computation." *Mech. Syst. Signal*

Process. 122 (May): 364–386. https://doi.org/10.1016/j.ymssp.2018.12.048.
Beaumont, M. A., W. Zhang, and D. J. Balding. 2002. "Approximate Bayesian computation in population genetics." *Genetics* 162 (4): 2025–2035. https://doi.org/10.1093/genetics/162.4.2025.
Beck, J. L., and L. S. Katafygiotis. 1998. "Updating models and their uncertainties. I: Bayesian statistical framework." *J. Eng. Mech.* 124 (4): 455–461. https://doi.org/10.1061/(ASCE)0733-9399(1998)124:4(455).
Beer, M. 2009. "Fuzzy probability theory." *Encycl. Complexity Syst. Sci.* 1 (1): 4047–4059. https://doi.org/10.1007/978-0-387-30440-3_237.
Beer, M., S. Ferson, and V. Kreinovich. 2013. "Imprecise probabilities in engineering analyses." *Mech. Syst. Signal Process.* 37 (1–2): 4–29. https://doi.org/10.1016/j.ymssp.2013.01.024.
Bernton, E., P. E. Jacob, M. Gerber, and C. P. Robert. 2019. "Approximate Bayesian computation with the Wasserstein distance." *J. R. Stat. Soc. B* 81 (2): 235–269. https://doi.org/10.1111/rssb.12312.
Betz, W., I. Papaioannou, and D. Straub. 2016. "Transitional Markov Chain Monte Carlo: Observations and improvements." *J. Eng. Mech.* 142 (5): 04016016. https://doi.org/10.1061/(ASCE)EM.1943-7889.0001066.
Bhattacharyya, A. 1943. "On a measure of divergence between two statistical populations defined by their probability distributions." *Bull. Calcutta Math. Soc.* 35 (Jun): 99–109.
Bhattacharyya, A. 1946. "On a measure of divergence between two multinomial populations." *Sankhya: Indian J. Stat.* 7 (4): 401–406.
Bi, S., M. Beer, S. Cogan, and J. E. Mottershead. 2023. "Stochastic model updating with uncertainty quantification: An overview and tutorial." *Mech. Syst. Signal Process.* 204 (Jun): 110784. https://doi.org/10.1016/j.ymssp.2023.110784.
Bi, S., M. Broggi, and M. Beer. 2019. "The role of the Bhattacharyya distance in stochastic model updating." *Mech. Syst. Signal Process.* 117 (Feb): 437–452. https://doi.org/10.1016/j.ymssp.2018.08.017.
Bi, S., K. He, Y. Zhao, D. Moens, M. Beer, and J. Zhang. 2022. "Towards the NASA UQ challenge 2019: Systematically forward and inverse approaches for uncertainty propagation and quantification." *Mech. Syst. Signal Process.* 165 (Feb): 108387. https://doi.org/10.1016/j.ymssp.2021.108387.
Bi, S., S. Prabhu, S. Cogan, and S. Atamturktur. 2017. "Uncertainty quantification metrics with varying statistical information in model calibration and validation." *AIAA J.* 55 (10): 3570–3583. https://doi.org/10.2514/1.J055733.
Bray, J. R., and J. T. Curtis. 1957. "An ordination of the upland forest communities of Southern Wisconsin." *Ecol. Monogr.* 27 (4): 325–349. https://doi.org/10.2307/1942268.
Bukatin, M., R. Kopperman, S. Matthews, and H. Pajoohesh. 2017. "Partial metric spaces." *Am. Math. Mon.* 116 (8): 708–718. https://doi.org/10.4169/193009709X460831.
Ching, J. Y., and Y. C. Chen. 2007. "Transitional Markov Chain Monte Carlo method for Bayesian model updating, model class selection, and model averaging." *J. Eng. Mech.* 133 (7): 816–832. https://doi.org/10.1061/(ASCE)0733-9399(2007)133:7(816).
Chrzaszcz, K., J. Jachymski, and F. Turobos. 2018. "On characterizations and topology of regular semimetric spaces." *Publ. Math. Debrecen* 93 (1–2): 87–105. https://doi.org/10.5486/PMD.2018.8049.
Crespo, L. G., S. P. Kenny, and D. P. Giesy. 2014. "The NASA Langley multidisciplinary uncertainty quantification challenge." In *Proc., 16th AIAA Non-Deterministic Approaches Conf.*, 1. Reston, VA: American Institute of Aeronautics and Astronautics. https://doi.org/10.2514/6.2014-1347.
de Angelis, M., and A. Gray. 2021. "Why the 1-Wasserstein distance is the area between the two marginal CDFs." Preprint, submitted November 5, 2011. https://doi.org/10.48550/arXiv.2111.03570.
de Carlo, E. C., B. P. Smarslok, and S. Mahadevan. 2016. "Segmented Bayesian calibration of multidisciplinary models." *J. Aerosp. Inf. Syst.* 54 (12): 3727–3741. https://doi.org/10.2514/1.J054960.
Dowding, K. J., M. Pilch, and R. G. Hills. 2008. "Formulation of the thermal problem." *Comput. Methods Appl. Mech. Eng.* 197 (29–32): 2385–2389. https://doi.org/10.1016/j.cma.2007.09.029.
Drieschner, M., Y. Petryna, S. Freitag, P. Edler, A. Schmidt, and T. Lahmer. 2021. "Decision making and design in structural engineering problems under polymorphic uncertainty." *Eng. Struct.* 231 (1): 111649. https://doi.org/10.1016/j.engstruct.2020.111649.
Dubois, D., L. Foulloy, G. Mauris, and H. M. Prade. 2004. "Probability-possibility transformations, triangular fuzzy sets, and probabilistic inequalities." *Reliab. Comput.* 10 (4): 273–297. https://doi.org/10.1023/B:REOM.0000032115.22510.b5.
Dubois, D., and H. M. Prade. 1988. *Possibility theory an approach to computerized processing of uncertainty.* Berlin: Springer.
Earle, C. J., L. A. Harris, J. H. Hubbard, and S. Mitra. 2003. "Schwarz's lemma and the Kobayashi and Carathéodory pseudometrics on complex Banach manifolds." *Kleinian Groups Hyperbolic 3-Manifolds* 219 (Feb): 363–384. https://doi.org/10.1017/CBO9780511542817.017.
Fang, S., S. Chen, Y. Lin, and Z. Dong. 2019. "Probabilistic damage identification incorporating approximate Bayesian computation with stochastic response surface." *Mech. Syst. Signal Process.* 128 (Aug): 229–243. https://doi.org/10.1016/j.ymssp.2019.03.044.
Ferson, S., V. Kreinovick, L. Ginzburg, D. S. Myers, and K. Sentz. 2003. *Constructing probability boxes and Dempster-Shafer structures*. Rep. No. SAND2002-4015. Livermore, CA: Sandia National Lab.
Ferson, S., W. Oberkampf, and L. Ginzburg. 2008. "Model validation and predictive capability for the thermal challenge problem." *Comput. Methods Appl. Mech. Eng.* 197 (29–32): 2408–2430. https://doi.org/10.1016/j.cma.2007.07.030.
Frechét, M. M. 1906. "Sur quelques points du calcul fonctionnel." *Rend. Del Circ. Mat. Di Palermo* 22 (1): 1–725. https://doi.org/10.1007/BF03018603.
Gelfand, A. E., and A. F. M. Smith. 1990. "Sampling-based approaches to calculating marginal densities." *J. Am. Stat. Assoc.* 85 (Jun): 398–409. https://doi.org/10.1080/01621459.1990.10476213.
Gilks, W. R., and P. Wild. 1992. "Adaptive rejection sampling for Gibbs sampling." *Appl. Stat.* 41 (2): 337–348. https://doi.org/10.2307/2347565.
Goodman, J., and J. Weare. 2010. "Ensemble samplers with affine invariance." *Commun. Appl. Math. Comput. Sci.* 5 (5): 65–80. https://doi.org/10.2140/camcos.2010.5.65.
Gotz, M., W. Graf, and M. Kaliske. 2015. "Structural design with polymorphic uncertainty models." *Int. J. Reliab. Saf.* 9 (2–3): 112–131. https://doi.org/10.1504/IJRS.2015.072715.
Graf, W., M. Gotz, and M. Kaliske. 2015. "Analysis of dynamical processes under consideration of polymorphic uncertainty." *Struct. Saf.* 52 (1): 194–201. https://doi.org/10.1016/j.strusafe.2014.09.003.
Gray, A., A. Wimbush, M. de Angelis, P. O. Hristov, D. Calleja, E. Miralles-Dolz, and R. Rocchetta. 2022. "From inference to design: A comprehensive framework for uncertainty quantification in engineering with limited information." *Mech. Syst. Signal Process.* 165 (Feb): 108210. https://doi.org/10.1016/j.ymssp.2021.108210.
Hastings, W. K. 1970. "Monte Carlo sampling methods using Markov Chains and their applications." *Biometrika* 57 (1): 97–109. https://doi.org/10.1093/biomet/57.1.97.
Hazra, I., M. D. Pandey, and M. I. Jyrkama. 2020a. "Estimation of flow-accelerated corrosion rate in nuclear piping system." *J. Nucl. Eng. Radiat. Sci.* 6 (1): 011106. https://doi.org/10.1115/1.4044407.
Hazra, I., M. D. Pandey, and N. Manzana. 2020b. "Approximate Bayesian computation (ABC) method for estimating parameters of the gamma process using noisy data." *Reliab. Eng. Syst. Saf.* 198 (Jun): 106780. https://doi.org/10.1016/j.ress.2019.106780.
He, L., Y. Liu, S. Bi, L. Wang, M. Broggi, and M. Beer. 2019. "Estimation of failure probability in braced excavation using Bayesian networks with integrated model updating." *Underground Space* 5 (4): 315–323. https://doi.org/10.1016/j.undsp.2019.07.001.
Helton, J. C. 1997. "Uncertainty and sensitivity analysis in the presence of stochastic and subjective uncertainty." *J. Stat. Comput. Simul.* 57 (1–4): 3–76. https://doi.org/10.1080/00949659708811803.
Helton, J. C., J. D. Johnson, and W. L. Oberkampf. 2004. "An exploration of alternative approaches to the representation of uncertainty in model predictions." *Reliab. Eng. Syst. Saf.* 85 (Aug): 39–71. https://doi.org/10.1016/j.ress.2004.03.025.
Hills, R. G., M. Pilch, K. J. Dowding, J. Red-Horse, T. L. Paez, I. Babuška, and R. Tempone. 2008. "Validation challenge workshop." *Comput.*

Methods Appl. Mech. Eng. 197 (29–32): 2375–2380. https://doi.org/10.1016/j.cma.2007.10.016.

Jachymski, J., and F. Turobos. 2020. "On functions preserving regular semimetrics and quasimetrics satisfying the relaxed polygonal inequality." *Rev. De La Real Acad. De Cienc. Exactas, Físicas y Nat. Ser. A. Mat.* 114 (3). https://doi.org/10.1007/s13398-020-00891-7.

Kantorovich, L. V. 1939. "Mathematical methods of organizing and planning production." *Manage. Sci.* 6 (4): 366–422. https://doi.org/10.1287/mnsc.6.4.366.

Katafygiotis, L. S., and J. L. Beck. 1998. "Updating models and their uncertainties. II: Model identifiability." *J. Eng. Mech.* 124 (4): 463–467. https://doi.org/10.1061/(ASCE)0733-9399(1998)124:4(463).

Khodaparast, H. H., and J. E. Mottershead. 2008. "Efficient methods in stochastic model updating." *Stochastic Model* 7 (8)|: 9.

Kitahara, M., S. Bi, M. Broggi, and M. Beer. 2021. "Bayesian model updating in time domain with metamodel-based reliability method." *J. Risk Uncertainty Eng. Syst. Part A: Civ. Eng.* 7 (3): 04021030. https://doi.org/10.1061/AJRUA6.0001149.

Kitahara, M., S. Bi, M. Broggi, and M. Beer. 2022a. "Distribution-free stochastic model updating of dynamic systems with parameter dependencies." *Struct. Saf.* 97 (Jul): 102227. https://doi.org/10.1016/j.strusafe.2022.102227.

Kitahara, M., S. Bi, M. Broggi, and M. Beer. 2022b. "Nonparametric Bayesian stochastic model updating with hybrid uncertainties." *Mech. Syst. Signal Process.* 163 (Jan): 108195. https://doi.org/10.1016/j.ymssp.2021.108195.

Kobayashi, S. 1976. "Intrinsic distances, measures and geometric function theory." *Bull. Am. Math. Soc.* 82 (3): 357–416. https://doi.org/10.1090/S0002-9904-1976-14018-9.

Kobayashi, S. 1984. "Projectively invariant distances for affine and projective structures." *Banach Center Publ.* 12 (1): 127–152. https://doi.org/10.4064/-12-1-127-152.

Kullback, S. 1997. *Information theory and statistics*. North Chelmsford, MA: Courier.

Kullback, S., and R. A. Leibler. 1951. "On information and sufficiency." *Ann. Math. Stat.* 22 (1): 79–86. https://doi.org/10.1214/aoms/1177729694.

Lintusaari, J., M. U. Gutmann, R. Dutta, S. Kaski, and J. Corander. 2017. "Fundamentals and recent developments in approximate Bayesian computation." *Syst. Biol.* 66 (Jun): 66–82. https://doi.org/10.1093/sysbio/syw077.

Lye, A. n.d. "Distance metrics and approximate Bayesian computation tutorial." Accessed August 31, 2023. https://github.com/Adolphus8/Approximate_Bayesian_Computation.git.

Lye, A. 2023. "Robust and efficient probabilistic approaches towards parameter identification and model updating." Ph.D. thesis, Institute for Risk and Uncertainty, Univ. of Liverpool, School of Engineering.

Lye, A., A. Cicirello, and E. Patelli. 2021. "Sampling methods for solving Bayesian model updating problems: A tutorial." *Mech. Syst. Signal Process.* 159 (Oct): 107760. https://doi.org/10.1016/j.ymssp.2021.107760.

Lye, A., A. Cicirello, and E. Patelli. 2022a. "An efficient and robust sampler for Bayesian inference: Transitional ensemble Markov Chain Monte Carlo." *Mech. Syst. Signal Process.* 167 (Mar): 108471. https://doi.org/10.1016/j.ymssp.2021.108471.

Lye, A., A. Cicirello, and E. Patelli. 2022b. "On-line Bayesian model updating and model selection of a piece-wise model for the creep-growth rate prediction of a nuclear component." In *Proc., 8th Int. Symp. on Reliability Engineering and Risk Management*, 67–74. Singapore: World Publishing.

Lye, A., A. Cicirello, and E. Patelli. 2023a. "On-line Bayesian inference for structural health monitoring under model uncertainty using sequential ensemble Monte Carlo." In *Proc., 13th Int. Conf. on Structural Safety and Reliability.* Shanghai, China: Shanghai Scientific and Technical Publishers.

Lye, A., A. Gray, M. de Angelis, and S. Ferson. 2023b. "Robust probability bounds analysis for failure analysis under lack of data and model uncertainty." In *Proc., 5th ECCOMAS Thematic Conf. on Uncertainty Quantification in Computational Sciences and Engineering*. Oslo, Norway: ECCOMAS Proceedia. https://doi.org/10.7712/120223.10345.19797.

Lye, A., M. Kitahara, M. Broggi, and E. Patelli. 2022c. "Robust optimization of a dynamic Black-box system under severe uncertainty: A distribution-free framework." *Mech. Syst. Signal Process.* 167 (Mar): 108522. https://doi.org/10.1016/j.ymssp.2021.108522.

Lye, A., L. Marino, A. Cicirello, and E. Patelli. 2023c. "Sequential ensemble Monte Carlo sampler for on-line bayesian inference of time-varying parameter in engineering applications." *J. Risk Uncertainty Eng. Syst. Part B: Mech. Eng.* 9 (3): 031202. https://doi.org/10.1115/1.4056934.

Marin, J. M., P. Pudlo, C. P. Robert, and R. J. Ryder. 2012. "Approximate Bayesian computational methods." *Stat. Comput.* 22 (6): 1167–1180. https://doi.org/10.1007/s11222-011-9288-2.

Mottershead, J. E., and M. I. Friswell. 1993. "Model updating in structural dynamics: A survey." *J. Sound Vib.* 167 (Jun): 347–375. https://doi.org/10.1006/jsvi.1993.1340.

Mottershead, J. E., M. Link, M. I. Friswell, and C. Schedlinski. 2021. "Model updating." In *Handbook of experimental structural dynamics*, 1–53. New York: Springer. https://doi.org/10.1007/978-1-4939-6503-8_18-2.

Nadjahi, K., V. de Bortoli, A. Durmus, R. Badeau, and U. Simsekli. 2020. "Approximate Bayesian Computation with the sliced-wasserstein distance." In *Proc., IEEE Int. Conf. on Acoustics, Speech and Signal Processing*. New York: IEEE.

Oberkampf, W. L., J. C. Helton, C. A. Joslyn, S. F. Wojtkiewicz, and S. Ferson. 2004. "Challenge problems: Uncertainty in system response given uncertain parameters." *Reliab. Eng. Syst. Saf.* 85 (Apr): 11–19. https://doi.org/10.1016/j.ress.2004.03.002.

Panaretos, V. M., and Y. Zemel. 2019. "Statistical aspects of Wasserstein distances." *Ann. Rev. Stat. Appl.* 6 (Mar): 405–431. https://doi.org/10.1146/annurev-statistics-030718-104938.

Park, I., and R. V. Grandhi. 2012. "Quantifying multiple types of uncertainty in physics-based simulation using Bayesian model averaging." *J. Aerosp. Inf. Syst.* 49 (5): 1038–1045. https://doi.org/10.2514/1.J050741.

Patelli, E., D. A. Alvarez, M. Broggi, and M. de Angelis. 2015. "Uncertainty management in multidisciplinary design of critical safety systems." *J. Aerosp. Inf. Syst.* 12 (1): 140–169. https://doi.org/10.2514/1.I010273.

Patelli, E., Y. Govers, M. Broggi, H. M. Gomes, M. Link, and J. E. Mottershead. 2017. "Sensitivity or Bayesian model updating: A comparison of techniques using the DLR-AIRMOD test data." *Arch. Appl. Mech.* 87 (May): 905–925. https://doi.org/10.1007/s00419-017-1233-1.

Ricotta, C., and J. Podani. 2017. "On some properties of the Bray-Curtis dissimilarity and their ecological meaning." *Ecol. Complexity* 31 (Sep): 201–205. https://doi.org/10.1016/j.ecocom.2017.07.003.

Rocchetta, R., M. Broggi, Q. Huchet, and E. Patelli. 2018a. "On-line Bayesian model updating for structural health monitoring." *Mech. Syst. Signal Process.* 103 (Mar): 174–195. https://doi.org/10.1016/j.ymssp.2017.10.015.

Rocchetta, R., M. Broggi, and E. Patelli. 2018b. "Do we have enough data? Robust reliability via uncertainty quantification." *Appl. Math. Modell.* 54 (Feb): 710–721. https://doi.org/10.1016/j.apm.2017.10.020.

Rockafellar, R. T., and R. J. B. Wets. 2010. *Variational analysis*. Berlin: Springer.

Roy, C. J., and W. L. Oberkampf. 2011. "A comprehensive framework for verification, validation, and uncertainty quantification in scientific computing." *Comput. Methods Appl. Mech. Eng.* 200 (Jun): 2131–2144. https://doi.org/10.1016/j.cma.2011.03.016.

Safta, C., K. Sargsyan, H. N. Najm, K. Chowdhary, B. Debusschere, L. P. Swiler, and M. S. Eldred. 2015. "Probabilistic methods for sensitivity analysis and calibration in the NASA challenge problem." *J. Aerosp. Inf. Syst.* 12 (1): 219–234. https://doi.org/10.2514/1.I010256.

Sheather, S. J., and M. C. Jones. 1991. "A reliable data-based bandwidth selection method for kernel density estimation." *J. R. Stat. Soc. B* 53 (Jul): 683–690. https://doi.org/10.1111/j.2517-6161.1991.tb01857.x.

Simoen, E., G. de Roeck, and G. Lombaert. 2015. "Dealing with uncertainty in model updating for damage assessment: A review." *Mech. Syst. Signal Process.* 56-57 (May): 123–149. https://doi.org/10.1016/j.ymssp.2014.11.001.

Smith, K. 2013. *Precalculus: A functional approach to graphing and problem solving*. Burlington, MA: Jones and Bartlett.

Smyth, M. B. 1988. "Quasi-uniformities: Reconciling domains with metric spaces." *Math. Found. Program. Lang. Semant.* 1 (Jun): 236–253. https://doi.org/10.1007/3-540-19020-1_12.

Steen, L. A., and J. A. Seebach. 1978. *Counterexamples in topology.* New York: Springer.

Sun, L., L. Zhu, W. Li, C. Zhang, and T. Balezentis. 2022. "Interval-valued functional clustering based on the Wasserstein distance with application to stock data." *Inf. Sci.* 606 (Aug): 910–926. https://doi.org/10.1016/j.ins.2022.05.112.

Turner, B. M., and T. V. Zandt. 2012. "A tutorial on approximate Bayesian computation." *J. Math. Psychol.* 56 (2): 69–85. https://doi.org/10.1016/j.jmp.2012.02.005.

Vaserstein, L. N. 1969. "Markov processes over denumerable products of spaces, describing large systems of automata." *Probl. Inf. Transm.* 5 (3): 64–72.

Vesentini, E. 1983. "Carathéodory distances and Banach algebras." *Adv. Math.* 47 (1): 50–73. https://doi.org/10.1016/0001-8708(83)90054-3.

Wang, C., L. Yang, M. Xie, M. Valdebenito, and M. Beer. 2023. "Bayesian maximum entropy method for stochastic model updating using measurement data and statistical information." *Mech. Syst. Signal Process.* 188 (Apr): 110012. https://doi.org/10.1016/j.ymssp.2022.110012.

Wilson, W. A. 1931. "On quasi-metric spaces." *Am. J. Math.* 53 (3): 675–684. https://doi.org/10.2307/2371174.

Worden, K. 2001. *Nonlinearity in structural dynamics: Detection, identification and modelling*. London: CRC Press.

Yager, R., M. Fedrizzi, and J. Kacprzyk. 1994. *Advances in the Dempster-Shafer theory of evidence*. New York: Wiley.

Zadeh, L. A. 1965. "Fuzzy sets." *Inf. Control* 8 (65): 338–353. https://doi.org/10.1016/S0019-9958(65)90241-X.

Zeng, Y., H. Wang, S. Zhang, Y. Cai, and E. Li. 2019. "A novel adaptive approximate Bayesian computation method for inverse heat conduction problem." *Int. J. Heat Mass Transfer* 134 (May): 185–197. https://doi.org/10.1016/j.ijheatmasstransfer.2019.01.002.

Zhao, W., L. Yang, C. Dang, R. Rocchetta, M. Valdebenito, and D. Moens. 2022a. "Enriching stochastic model updating metrics: An efficient Bayesian approach using Bray-Curtis distance and an adaptive binning algorithm." *Mech. Syst. Signal Process.* 171 (May): 108889. https://doi.org/10.1016/j.ymssp.2022.108889.

Zhao, W., L. Yang, and P. Wang. 2022b. "Stochastic model calibration using the Bray-Curtis distance-based uncertainty quantification metric." In *Proc., 12th Int. Conf. on Quality, Reliability, Risk, Maintenance, and Safety Engineering*, 1315–1320. London: Institution of Engineering and Technology. https://doi.org/10.1049/icp.2022.3050.

Zhu, C., W. Tian, B. Yin, Z. Li, and J. Shi. 2020. "Uncertainty calibration of building energy models by combining approximate Bayesian computation and machine learning algorithms." *Appl. Energy* 268 (Aug): 115025. https://doi.org/10.1016/j.apenergy.2020.115025.